Robotics and Autonomous Systems 156 (2022) 104207

Contents lists available at ScienceDirect

Robotics and Autonomous Systems

journal homepage: www.elsevier.com/locate/robot

A unified Lloyd-based framework for multi-agent collective behaviours

Manuel Boldrer [a,*], Luigi Palopoli [b], Daniele Fontanelli [c]

[a] Faculty of Mechanical, Maritime, and Materials Engineering, Delft University of Technology, Mekelweg 2, 2628 CD Delft, The Netherlands
[b] Department of Information Engineering and Computer Science, University of Trento, 38122, Trento, Italy
[c] Department of Industrial Engineering, University of Trento, 38122, Trento, Italy

ARTICLE INFO

Article history:
Received 13 March 2021
Received in revised form 7 July 2022
Accepted 13 July 2022
Available online 22 July 2022

Keywords:
Distributed control
Collective behaviours
Lloyd-based algorithms

ABSTRACT

Different authors have addressed a number of problems in the area of distributed control proposing convincing solutions to specific problems such as static coverage, dynamic coverage/exploration, rendezvous, flocking, formation control. However, a major limitation of problem-specific approaches is a fundamental lack of flexibility when the group meets unexpected conditions and has to change its goal on the fly. In this paper, we show that a large class of distributed control problems can be cast into a general framework based on the adoption of the Lloyd methodology. The adoption of a unified framework enables efficient solutions for the specific problems guaranteeing at the same time important safety and functional properties and a large degree of flexibility in the execution of group tasks. The paper sets the theoretical basis for this development and proves the efficacy of the proposed solutions through extensive simulations and experimental results.

1. Introduction

Distributed coordination and control of multi-robot systems is a very active research area and is attracting interest from different scientific communities. The main idea is to define distributed strategies, in which each robot senses its surroundings and takes a decision coordinating with its neighbours. The combination of these different local decisions produces a collective behaviour (also called emergent behaviour) for the system as a whole [1]. The problem of distributed control is about designing local control laws such that the emerging collective behaviour fulfils the desired control goals. The complexity of distributed control design is compensated by its undisputed benefits in terms of communication, sensing and computing power requirements, flexibility and robustness. In the following, we are going to review some of the most important problems that can be addressed using distributed control of multi-robot systems.

Static Coverage. The problem of static coverage amounts to finding a deployment for a group of robots such that a given area is optimally covered by their sensors. A seminal paper by Cortes et al. [2] sets up the problem for convex environments. The authors exploit a technique based on Voronoi partitions and first proposed by Lloyd [3] for the optimal design of quantisers, and adopt a gradient descent strategy that provably converges to the centroidal Voronoi configurations. Extensions to non-convex environments have been proposed by different authors. A combination of the Lloyd algorithm and the *TangentBug* method is proposed by Breitenmoser et al. [4], while Pimenta et al. [5] use geodesic Voronoi tessellation in order to account for the heterogeneous range of the sensors embedded on the robots. Stergiopoulos et al. [6] compare Euclidean and geodesic sensing discs and also Euclidean and geodesic Voronoi partitioning. In [7–9] the authors proposed coverage solutions based on the visibility set to deal with non-convex spaces. Other approaches are based on potential fields [10], time-inverted Kuramoto dynamics [11], on the maximisation of the joint detection probabilities of random events [12] or address specific application areas [13].

Dynamic Coverage. When the number of agents is not sufficient to statically cover all the mission space, exploration algorithms featuring dynamic coverage are in order. In 1997, Yamauchi [14] introduced the concept of frontier, which is a region between the unexplored space and the open space that the robot moves towards to increase its knowledge of the environment. The idea of the frontier-based navigation was extended by the same author to the case of multi-robot teams [15]. Effective multi-robot exploration strategies have been proposed by Burgard et al. [16] using a decision-theoretic approach, in which frontiers are used as a means to coordinate the robots. Franchi et al. in [17] present a decentralised cooperative exploration strategy using sensor-based random graph. A behavioural approach is adopted by Cepeda et al. [18]: the authors combine four simple behaviours to obtain a complex emergent behaviour which results into the exploration of unknown environments by a group of robots. Furthermore, an interesting interpretation of the exploration problem is proposed by Semnani et al. [19], who introduce the concept of

* Corresponding author.
E-mail addresses: m.boldrer@tudelft.nl (M. Boldrer), luigi.palopoli@unitn.it (L. Palopoli), daniele.fontanelli@unitn.it (D. Fontanelli).

https://doi.org/10.1016/j.robot.2022.104207

anti-flocking and semi-flocking. Schwager et al. [20] propose a bio-inspired control strategy for coverage and exploration of a convex area. Haumann et al. [21] combine the frontier-based strategy with the Voronoi partition, thus ensuring collision avoidance between robots, due to the properties of the Voronoi partition [22]. Franco et al. [23] proposes a persistent coverage algorithm based on the combination of local and global strategies in order to guarantee full coverage. In the same line of work, Mellone et al. [24] provide a distributed control law for persistent coverage of a team of heterogeneous robots in a structured environment, while Zhou et al. [25] propose an event-driven solution for one-dimensional persistent monitoring problems. Other solutions for one-dimensional persistent monitoring are proposed in [26–28].

Connectivity Maintenance. When a group of robots moves, some of the agents in the team could be delayed and lose connection with the group. With a motion strategy that is connectivity-preserving this situation never occurs and the communication graph is always connected. Sabattini et al. [29] ensure connectivity maintenance by relying on a gradient descent based algorithm and a decentralised estimation of the second smallest eigenvalue of the Laplacian matrix (i.e. the algebraic connectivity). De Gennaro et al. [30] seek to maximise the algebraic connectivity in a decentralised way, when no obstacle is in the workspace, while Stump et al. [31] extend their solution to the presence of obstacles. A similar approach is adopted by Kim et al. [32], who set up a semi-definite programming solution to solve the problem. Schuresko et al. [33] deal with connectivity maintenance accounting for imperfect information in the communication system, while Zavlanos et al. in [34] present an algorithm able to preserve k-hop connectivity. The same research group proposes a theoretical framework conceived for connectivity graph control [35], and a network topology-based solution with no restrictions on the desired connectivity specification [36].

Navigation. Navigation strategies for multi-robot groups were pioneered by Reynolds [37], who introduced a model of polarised, non-colliding aggregate motion (i.e. flocking), and by Olfati-Saber [38], who set up a theoretical framework for the design and analysis of flocking algorithms. Olfati-Saber, in particular, proposed a potential-based method that forces the robot to converge to a lattice structure (i.e. formation). There are plenty of literature results on multi-robot navigation, a large part of these being derived from the works of Reynolds and Olfati-Saber, however a complete survey is beyond the scope of this paper.

Rendezvous. The rendezvous problem can be described in the following terms: define a control strategy such that all the robots converge to the same point. To solve this problem, Ando et al. introduce the circumcenter algorithm in [39], which was later extended by different authors [40,41]. Dimarogonas et al. [42] propose a decentralised feedback control strategy that steers a set of nonholonomic agents to a rendezvous pose. Ji et al. [43] achieve rendezvous through nonlinear feedback control based on weighted Laplacian matrix. To the best of our knowledge, the rendezvous problem in non-convex spaces has been rarely addressed. The most relevant existing solutions are the Perimeter Minimising Algorithm for non-convex connected spaces [44] or potential field-based approaches [45].

Paper Contribution. In this paper, we propose a unified framework for the whole class of the distributed control problems mentioned above. The mainstay of our methodology is the Lloyd algorithm [3]. With respect to previous papers that used this approach, we combine two key features. First, we modify the geometry of the Voronoi partitions to account for visibility and communication constraints as well as for the physical encumbrance of the agents. Second, we change dynamically the attractiveness of the different areas inside the Voronoi partitions to push the agents towards the execution of dynamic goals. These two features were used in a different context in previous papers [46,47]. In our framework, their combination allows us to synthesise a family of different control algorithms within the same framework. Specifically, we provide:

(1) An adaptive static coverage algorithm dealing with non-convex environments. Preliminary results on static coverage were provided in our previous paper [7], but we did not offer any formal proof of safety and, in some pathological conditions, the agents could be trapped in local minima. The solution presented in this paper comes with a formal proof of safety, mitigates the problem of local minima and offers a test, in the case of homogeneous sensors, to decide if the environment has been fully covered;
(2) A comprehensive solution for dynamic coverage that considers three different scenarios: i. memoryless robots, ii. robots with memory of past positions, iii. robots with memory of past positions and exchanging information. Unlike the frontier-based methods [14], our solution does not require the support of planning algorithms to reach the frontiers;
(3) A novel motion control algorithm for connectivity maintenance;
(4) A group navigation technique that switches between a *flocking* behaviour, i.e., the robots maintain a loose formation [48,49], and a constrained formation behaviour, where each robot has to keep a fixed distance from its neighbours;
(5) A rendezvous algorithm that operates in generic non-convex environments (e.g., a room cluttered with obstacles).

As well as being relevant in their own rights, these different algorithms are rooted in the same conceptual model, are formulated and analysed uniformly and share two properties of the greatest importance: they secure collision and obstacle avoidance and they can operate with heterogeneous sensors.

The paper is organised as follows. In Section 2 we lay down the basic pillars upon which the rest of the paper is built upon. Section 3 uses the Lloyd algorithm and act on the Voronoi cell geometry to ensure collision avoidance, adaptive static coverage as well as connectivity maintenance, while Section 4 act on the cell densities to ensure dynamic coverage, navigation and rendezvous. The qualitative and quantitative results are offered both in simulation and experimentally in Sections 5 and 6. The paper ending comments are reported in Section 7, where the future research directions and developments are also discussed.

2. Problem formulation and solution overview

In this section, we formalise the different control problems and we briefly review the results of Lloyd that underpin the unified framework proposed in this paper.

2.1. Problem formulation

Given the mission space $\mathcal{Q} \subset \mathbb{R}^2$, the obstacle space $\mathcal{O} \subset \mathbb{R}^2$ and a finite number n of robotic agents with initial position $p_i(0) \in \mathcal{Q}\ \forall i = 1 \dots n$, our goal is to design control laws that operate through local interactions so that the collective (global) behaviour of the group fulfils one of the following goals:

- *Static coverage*: the system reaches a stable configuration that deploys the robot in the mission space so that a coverage metric is optimised;

- *Connectivity maintenance*: given an initial connectivity graph defined by edges and vertices, the robots move so that if two vertices (robots) are linked through an edge (connectivity constraint), they remain connected, i.e. if a connectivity constraint is imposed between two robots, each robot moves in order to respect the constraint and does not leave the communication set of its neighbour(s);
- *Dynamic coverage*: the robot motion strategy guarantees that the entire mission space is covered by the sensing range of the robots in finite time; in case the number of robots is not sufficient to statically cover the whole mission space, we need a dynamic solution such that each location is covered at least in some time intervals;
- *Navigation*: (i) Flocking: move the robotic agents from the starting positions $\mathcal{P} = \{p_1(0), p_2(0), \dots, p_n(0)\}$ to the goal positions $\mathcal{E} = \{e_1, e_2, \dots, e_n\}$, keeping the pairwise distance between agents smaller than a specified amount; (ii) Formation: move the robotic agents from the starting positions $\mathcal{P} = \{p_1(0), p_2(0), \dots, p_n(0)\}$ to the goal positions $\mathcal{E} = \{e_1, e_2, \dots, e_n\}$, keeping constant pairwise distance between the agents;
- *Rendezvous*: each robot of the system converges to the same rendezvous position.

For all these problems, we require to:

- Avoid collisions with obstacles;
- Avoid collisions between the robots in the group;
- Deal with heterogeneous sensing ranges.

We assume a single integrator dynamics $\dot{p}_i = u_i$, for each agent in the scene (i.e., we can independently set the velocities along with the two coordinates). In the following, we will use the terms "robot" or "agent" with the same meaning.

2.2. Lloyd-based algorithms

More than a decade ago Cortes et al. [2] proposed a Lloyd-based solution to solve the coverage problem in a distributed way. Their idea was to define a coverage cost function

$$J_{\text{cov}}(p, \mathcal{V}) = \sum_{i=1}^{n} \int_{\mathcal{V}_i} \|q - p_i\|^2 \varphi(q) dq, \tag{1}$$

where $p = [p_1, \dots, p_n]^T$, $p_i = [x_i, y_i]^T$ is the position of the i-th agent, $q \in \mathcal{Q}$ are the points belonging to the mission space, $\varphi(q)$ is the probability density function that weighs the relevance of point q, and $\mathcal{V}_i$ is the Voronoi cell associated with the i-th agent,

$$\mathcal{V}_i(p) = \left\{ q \in \mathcal{Q} \mid \|q - p_i\| \leq \|q - p_j\|, \forall j \neq i \right\}. \tag{2}$$

By following the gradient descent (i.e. $-\frac{\partial J_{\text{cov}}(p,\mathcal{V})}{\partial p_i}$), and assuming the single integrator dynamics $\dot{p}_i = u_i$, Cortes et al. obtained the following proportional control law

$$\dot{p}_i(\mathcal{V}_i) = -k_p \left(p_i - C_{\mathcal{V}_i}\right), \tag{3}$$

where $k_p > 0$ is a tuning parameter, and $C_{\mathcal{V}_i} = [C^x_{\mathcal{V}_i}, C^y_{\mathcal{V}_i}]^T$ is the centroid position computed over the i-th Voronoi cell. They proved that each agent converges asymptotically to its Voronoi centroid position and the overall system achieves an optimal deployment for the coverage problem. They showed this fact by using $J_{\text{cov}}(p, \mathcal{V})$ as a Lyapunov function:

$$\begin{aligned} \frac{d}{dt} J_{\text{cov}}(p, \mathcal{V}) &= \sum_{i=1}^{n} \frac{\partial}{\partial p_i} J_{\text{cov}}(p, \mathcal{V}) \dot{p}_i \\ &= \sum_{i=1}^{n} 2m_i (p_i - C_{\mathcal{V}_i})^T (-k_p (p_i - C_{\mathcal{V}_i})) \\ &= -2k_p \sum_{i=1}^{n} m_i \|p_i - C_{\mathcal{V}_i}\|^2 \end{aligned} \tag{4}$$

where $m_i = \int_{\mathcal{V}_i} \varphi(q) dq$. The convergence to the central Voronoi tessellation is a consequence of LaSalle's invariance principle.

The framework proposed in this paper relies on the Lloyd-based relations (1), (2) and (3). It retains the simplicity and the effectiveness of the approach of [2] but it applies to a far more general and challenging category of distributed control problems.

2.3. Unified Lloyd-based distributed coordination

The general control law to solve the problems described in Section 2.1 can be written as follows:

$$\begin{aligned} \dot{p}_i(\mathcal{A}_i, \mathcal{Z}_i) = \underset{\nu}{\operatorname{argmin}} \left(\left\| \nu + k_p(p_i - C_{\mathcal{A}_i}) - k_e \frac{\dot{C}_{\mathcal{A}_i}}{\|\dot{C}_{\mathcal{A}_i}\|} \right\| \right), \\ \text{s.t. } \nu \in \text{int}(\hat{\mathcal{T}}(\mathcal{Z}_i, p_i)) \text{ if } p_i \in \partial \mathcal{Z}_i \end{aligned} \tag{5}$$

where k_p and k_e are tuning parameters, $\text{int}(\hat{\mathcal{T}}(\mathcal{Z}_i, p_i))$ is the interior of the sequential Bouligant tangent cone [50] (also called contingent cone) to $\mathcal{Z}_i$ at p_i and $\partial \mathcal{Z}_i$ is the boundary of the $\mathcal{Z}_i$ set. In practice, the constraint in (5) enforces the i-th agent to belong to the cell $\mathcal{Z}_i$, which is a fundamental requirement to prove safety and functional properties. By properly choosing the sets $\mathcal{A}_i$, $\mathcal{Z}_i$ and the density function $\varphi(q)$ used to compute the centroid $C_{\mathcal{A}_i}$ of $\mathcal{A}_i$, the system emergent behaviours fulfil one or more of the tasks summarised in Section 2.1. As a particular case, when (5) is used with just one parameter, e.g. $\dot{p}_i(\mathcal{A}_i)$, it is implicitly intended as $\dot{p}_i(\mathcal{A}_i, \mathcal{A}_i)$. Notice that (3) is then $\dot{p}_i(\mathcal{V}_i)$ in (5) with $k_e = 0$.

3. Cell geometry adaption

In this section, we show that by simply operating on the cell geometry, we can extend the applicability of Lloyd-based solution to a far greater class of problems than the coverage maximisation of convex spaces recalled in Section 2.

3.1. Collision avoidance between agents

In the model discussed in Section 2, the agents were approximated as particles. However, in many applications, their encumbrance must be considered. For a single agent having to avoid static obstacles, the solution can simply be to inflate the obstacles in order to account for its physical encumbrance. Collision avoidance between agents requires more effort.

Previous approaches for homogeneous agent dimensions [5] and for heterogeneous agent dimensions [51], provide useful ideas. Let us consider Fig. 1 and assume that the i-th agent can be approximated with a circle of radius δ_i. Hence, the Voronoi tessellation can be modified as follows

$$\tilde{\mathcal{V}}_i = \begin{cases} \left\{ q \in \mathcal{Q} \mid \|q - p_i\| \leq \|q - p_j\| \right\}, \text{if } \Delta_{ij} \leq \frac{\|p_i - p_j\|}{2}, \\ \left\{ q \in \mathcal{Q} \mid \|q - p_i\| \leq \|q - \tilde{p}_j\| \right\}, \text{otherwise}, \end{cases} \tag{6}$$

where $\Delta_{ij} = \delta_j + \delta_i$ and $\tilde{p}_j = p_j + 2\left(\Delta_{ij} - \frac{\|p_i - p_j\|}{2}\right) \frac{p_i - p_j}{\|p_i - p_j\|}$. By considering the cell partition (6) and by applying $\dot{p}_i(\tilde{\mathcal{V}}_i)$ as defined in (3) (i.e., $k_e = 0$ in (5)), the agents do not collide, as shown in the following.

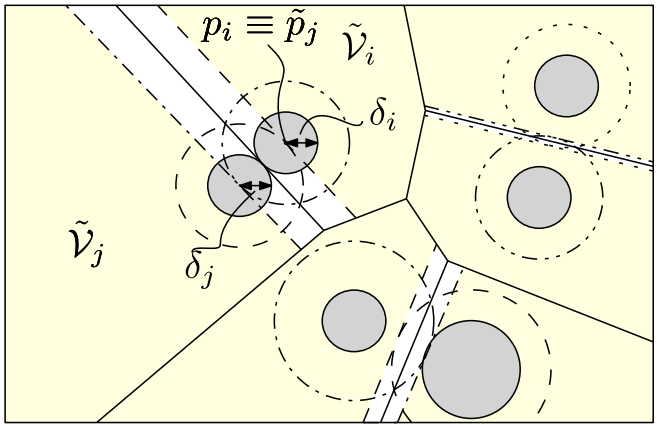

Fig. 1. (a) Voronoi set $\tilde{\mathcal{V}}_i$ defined in (6) to take into account the agents' encumbrance.

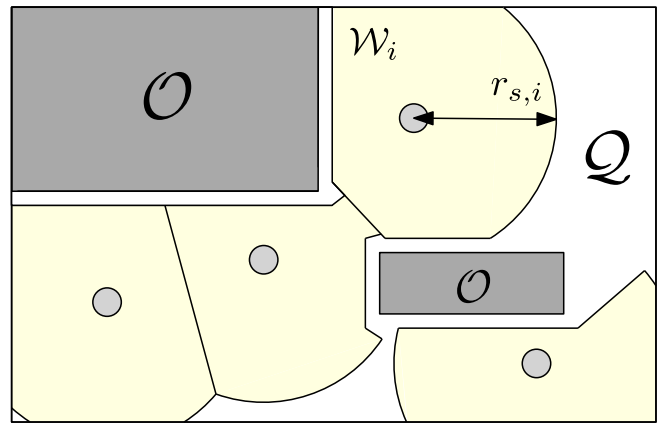

Fig. 2. Voronoi-Visible set $\mathcal{W}_i$ defined in (7) with static obstacles inflated.

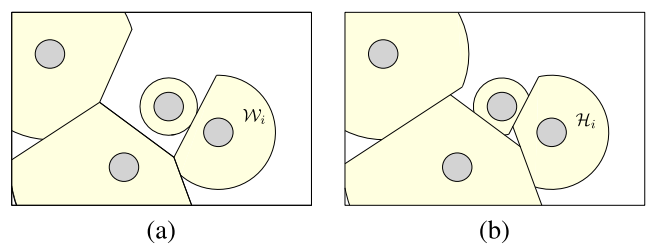

Fig. 3. In (a) the Voronoi-Visible set $\mathcal{W}_i$, defined in (7), while in (b) the partition $\mathcal{H}_i \cap \mathcal{S}_i$ defined in (9), (8) to take into account the heterogeneous sensing ranges.

Theorem 1 (*Collision Avoidance*)**.** *Given the mission space $\mathcal{Q}$, by imposing to agent i to always remain in its cell $\tilde{\mathcal{V}}_i$, e.g by imposing $\dot{p}_i(\tilde{\mathcal{V}}_i)$ as defined in (3), if the agents position at time $t = 0$ satisfies $\|p_i(0) - p_j(0)\| > \Delta_{ij}$, collision avoidance between agents is guaranteed $\forall t \geq 0$.*

Proof. Consider the cell partition in (6) (see Fig. 1) and the controlled dynamics $\dot{p}_i(\tilde{\mathcal{V}}_i)$. When $d_{ij} = \|p_i(t) - p_j(t)\| > \Delta_{ij}$ (i.e. no collision), two cases can occur: $\dot{d}_{ij} \geq 0$ and $\dot{d}_{ij} < 0$. The former case is inherently safe. On the contrary, if $\dot{d}_{ij} < 0$ the condition $d_{ij} = \Delta_{ij}$ (i.e. close to collision) could eventually be reached. In this condition, both the scalar products become non positive by construction, i.e., $\langle p_j - p_i, \dot{p}_i(\tilde{\mathcal{V}}_i)\rangle \leq 0$ and $\langle p_i - p_j, \dot{p}_j(\tilde{\mathcal{V}}_j)\rangle \leq 0$, which implies $\dot{d}_{ij} \geq 0$. As a consequence, the robots will not get any closer. □

3.2. Obstacle avoidance

The solution discussed next brings about important improvements on our previous work [7] and provides formal proof of its safety properties. The idea was to generalise the approach of Cortes et al. [2] to non-convex spaces. We define the Voronoi-Visibility set

$$\mathcal{W}_i = \{\mathcal{V}_i \cap \mathcal{S}_i\}, \tag{7}$$

where the Visibility set $\mathcal{S}_i$ associated with the i-th agent (see Fig. 2), is defined as

$$\mathcal{S}_i = \{q \in \mathcal{Q} \,|\, p_i - \gamma\,(p_i - q) \notin \mathcal{O}\} \cap \left\{q \in \mathcal{Q} \,|\, \|q - p_i\| \leq r_{s,i}\right\}, \tag{8}$$

$\forall \gamma \in [0, 1]$, where $r_{s,i} \in (0, R_{s,i}]$ is a tunable sensing radius, which lives in the range between zero and the maximum sensing range $R_{s,i}$ of the i-th agent, while $\mathcal{O}$ is the obstacle space that each agent has to avoid.

The fact that the centroid position falls inside the cell is not in general guaranteed, since the Voronoi-Visible set is no more necessarily convex. To overcome this problem, we impose that the velocity selected by the controller constraints the agent within the cell, by choosing $k_e = 0$ and $\dot{p}_i(\mathcal{W}_i)$ in (5). Notice that by intersecting $\mathcal{W}_i$ (or any arbitrary set) with $\tilde{\mathcal{V}}_i$ and imposing $\dot{p}_i(\mathcal{W}_i \cap \tilde{\mathcal{V}}_i)$, Theorem 1 still holds true.

Theorem 2 (*Obstacle Avoidance*)**.** *Given the mission space $\mathcal{Q}$, and the obstacle space $\mathcal{O}$, by using the control law $\dot{p}_i(\mathcal{W}_i)$ with $k_e = 0$ given by (5), if the i-th agent position at time t_0 satisfies $p_i(0) \in \mathcal{Q}$, obstacle avoidance is guaranteed.*

Proof. The i-th agent velocity $\dot{p}_i(\mathcal{W}_i)$ in (5) determines $p_i(t) \in \mathcal{W}_i \subseteq \mathcal{S}_i$, $\forall t$, by construction. As a result, the agents will never enter in the obstacle space $\mathcal{O}$ along the controlled trajectories, since $\mathcal{S}_i \cap \mathcal{O} = \emptyset$ by definition (8). □

Notice that, As we mentioned before, the encumbrance of the agents can be managed by inflating the obstacle dimensions of an amount equal to the occupancy radius of the agent.

3.3. Heterogeneous sensing ranges

When the sensing ranges of the agents differ by a significant amount, the Voronoi partitioning proposed above does not necessarily produce a good coverage. Existing approaches to deal with this issue are the power-weighted Voronoi diagram (PWVD) [52] and the multiplicatively weighted Voronoi diagram (MWVD) [53]. Both approaches have an important limitation: they either disrupt the cell convexity when moving in free space or construct a cell that does not contain the agent p_i, which may not be desirable in our framework. This problem can be directly addressed by introducing a weight accounting for the sensing range in Voronoi partitions. By defining $\alpha_{ij} = \operatorname{atan}\left(\frac{y_j - y_i}{x_j - x_i}\right)$, our weighted Voronoi tessellation is constructed as follows

$$\mathcal{H}_i = \left\{q \in \mathcal{Q} \,|\, w_{ij}(q) < \frac{r_{s,i}}{r_{s,i} + r_{s,j}} \|p_i - p_j\|\right\} \cap \{q \,|\, \|w\| < R_{s,i}\}, \tag{9}$$

where $w_{ij}(q) = [\cos\alpha_{ij},\ \sin\alpha_{ij}](q - p_i)$. A graphical representation of the differences induced by (9) is depicted in Fig. 3, while its advantages in the static coverage algorithm is clearly shown in Fig. 4. Notice that the first set in (9) is a generalisation of the Voronoi partition $\mathcal{V}_i$, indeed $r_{s,i} = r_{s,j} \implies \{q \in \mathcal{Q} \mid w_{ij}(q) < \frac{1}{2}\|p_i - p_j\|\} \equiv \mathcal{V}_i$.

Trivially, the safety properties stated in Theorem 1 (absence of collisions between the agents) and in Theorem 2 (absence of collisions with static obstacles) are preserved by considering either

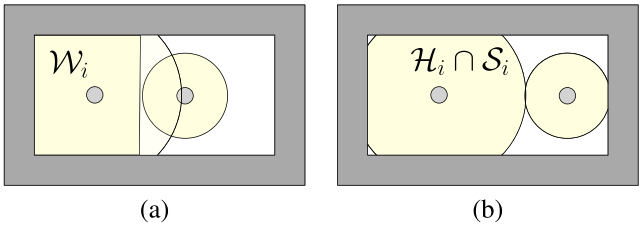

Fig. 4. In (a) the result of the Lloyd algorithm by considering the Voronoi-Visible set $\mathcal{W}_i$, defined in (7), while in (b) the Lloyd algorithm final configuration by considering the partition $\mathcal{H}_i \cap \mathcal{S}_i$ to take into account the heterogeneous sensing ranges.

the intersection $\mathcal{S}_i \cap \tilde{\mathcal{V}}_i$ or $\mathcal{S}_i \cap \tilde{\mathcal{H}}_i$, $\forall i$, in the centroid computation, where $\tilde{\mathcal{H}}_i$ is the analogous of (6) for the heterogeneous Voronoi partition (9).

Remark 1 (*Distributed Algorithm*)**.** The proposed algorithm can be computed in a fully distributed manner, since each agent has to compute quantities that depend only on local information. Indeed, the Voronoi diagram in (2) has not to be computed entirely by each agent, i.e. accounting $\forall j \neq i$, but just $\forall j \in \mathcal{N}_i$, where the neighbours set $\mathcal{N}_i$ is equal to

$$\mathcal{N}_i = \{j \mid p_j \in \mathcal{S}_i^\star\},$$

where $\mathcal{S}_i^\star$ is defined as in (8), with $r_{s,i}$ equal to the communication radius i.e., $r_{s,i} = R_{c,i}$.

3.4. Adaptive static coverage in non-convex spaces

The static coverage solutions described above are based on the control law (3), which is based on a gradient-descent idea. As a consequence, configurations in which the robots remain trapped in a local minimum cannot be ruled out, with an important impact on the level of coverage eventually achieved. A possible way to mitigate this problem is to enable the agents to "push" each other towards the free space. This effect can be obtained by using a weighted Voronoi partition as in (9) in which the sensing radius $r_{s,i}$ is artificially manipulated. To this end, let us consider the following dynamics,

$$\dot{r}_{s,i} = \begin{cases} k_0(\underline{r}_{s,i} - r_{s,i}), \text{ if } \exists\, q \in \mathcal{W}_i \mid \|q - p_i\| = R_{s,i}, \\ k_1(R_{s,i} - r_{s,i}), \text{ otherwise,} \end{cases} \tag{10}$$

where $R_{s,i}$ is the actual sensing range, while $\underline{r}_{s,i} > 0$ is a lower bound and is a design parameter along with the two constants $k_0 > 0$ and $k_1 > 0$. The rationale of (10), once combined with (9), is to inflate the cell (by increasing $r_{s,i}$) when it is constrained by the presence of other agents or obstacles (i.e., when the points in the set $\mathcal{W}_i$ do not reach the boundary of the sensing range $R_{s,i}$), or deflate it when there is some free space (hence, leaving space for the inflation of the other agents). In Fig. 5, we depict the "pushing" effect of the adaptive law. The adaptive control law obtained combining the equation $\dot{p}_i(\mathcal{S}_i \cap \tilde{\mathcal{H}}_i)$ with $k_e = 0$ in (5) with the adaptive rule (10) does not guarantee the absence of local minima. However, as shown in Section 5, its coverage performance is much better than its non-adaptive counter-part.

3.5. Coverage test

The performance of the coverage algorithms introduced above and the presence of local minima are highly influenced by the environment configuration and by the initial conditions of the agents, i.e. the same area may require a different number of agents depending on the position and the shape of the obstacles.

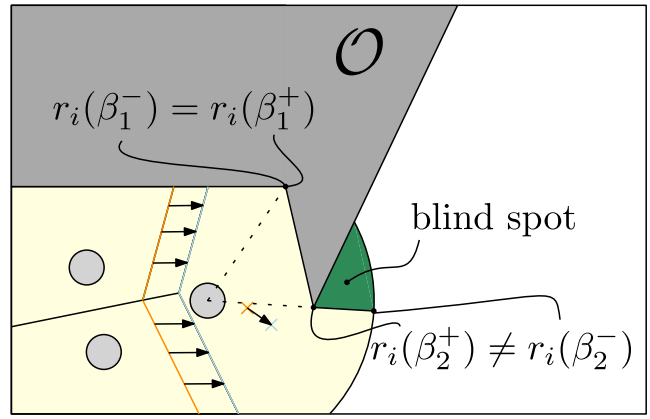

Fig. 5. Comparison between static coverage tessellation (i.e using $\mathcal{W}_i$, in orange) and the adaptive static coverage tessellation (i.e. using $\mathcal{S}_i \cap \mathcal{H}_i$ and the adaptive law (10), in blue). The crosses are the corresponding centroid positions. We also depict an example of "blind spot" for the i-th agent in direction $\theta = \beta_2$ (i.e. $r_i(\beta_2^-) \neq r_i(\beta_2^+)$). (For interpretation of the references to colour in this figure legend, the reader is referred to the web version of this article.)

Unfortunately, determining the minimum number of agents required to reach the full coverage given the initial configuration is a too challenging problem, unless restrictive assumptions about the obstacles' shapes are considered. However, we will now show a sufficient condition to test if the area has been fully covered in the case of homogeneous sensing ranges.

Intuitively, to cover the mission space, two conditions have to be met: 1. each Voronoi cell falls entirely within the visibility range of the agent that it contains, i.e., $\forall q \in \mathcal{V}_i$, we have $\|q - p_i\| \leq r_{s,i}$, $\forall i$, 2. all the points within the mission space that belong to a Voronoi cell are visible to the agent, i.e., $\forall q \in \{\mathcal{V}_i \setminus \mathcal{O}\}$, it holds $q \in \mathcal{S}_i$, $\forall i$. In order to formalise the second condition, which we will refer to as absence of "blind spots", let us define $\mathcal{B}(\mathcal{S}_i \cap \mathcal{V}_i)$ as the points belonging to the border of the i-th Voronoi-Visible set. We can provide a mathematical definition of this set using polar coordinates $\left(r_i^{\mathcal{S}_i \cap \mathcal{V}_i}, \theta\right)$ with p_i as centre, where the distance $r_i^{\mathcal{S}_i \cap \mathcal{V}_i}$ of each point is a function of the angle θ. To this end, we first consider (8) and the set $\mathcal{R}(\mathcal{S}_i, \theta) = \{r_i(\theta) \in \mathbb{R} \mid p_i + r_i(\theta)[\cos\theta \;\; \sin\theta]^T \in \mathcal{S}_i\}$. The radius $r_i^{\mathcal{S}_i}(\theta)$, defined $\forall \theta \in [0, 2\pi)$ as $r_i^{\mathcal{S}_i}(\theta) = \max_{r_i(\theta)} \{r_i(\theta) \in \mathcal{R}(\mathcal{S}_i, \theta)\}$ defines the boundary $\mathcal{B}(\mathcal{S}_i)$. Due to the fact that $\mathcal{V}_i$ is a convex set, it follows that $\forall \theta \in [0, 2\pi)$ there exists a unique point on the boundary associated within $\mathcal{R}(\mathcal{S}_i \cap \mathcal{V}_i, \theta)$, with distance from p_i given by the radius $r_i^{\mathcal{S}_i \cap \mathcal{V}_i}(\theta)$. As a consequence, it is possible to express the set $\mathcal{B}(\mathcal{S}_i \cap \mathcal{V}_i)$ as $\mathcal{B}(\mathcal{S}_i \cap \mathcal{V}_i) = \{p_i + r_i^{\mathcal{S}_i \cap \mathcal{V}_i}(\theta)[\cos\theta \;\; \sin\theta]^T\}_{\theta=0}^{2\pi}$. This definition is instrumental to check for the existence of "blind spots" (see Fig. 5 for a graphical representation of such a spatial region).

Proposition 1 (*Blind Spots*)**.** *A blind spot for the i-th agent exists when*

$$\lim_{\theta \to \beta^-} r_i^{\mathcal{S}_i \cap \mathcal{V}_i}(\theta) \neq \lim_{\theta \to \beta^+} r_i^{\mathcal{S}_i \cap \mathcal{V}_i}(\theta), \quad \forall \beta \in [0, 2\pi), \tag{11}$$

Proof. We first notice that each cell defined by $\mathcal{S}_i \cap \mathcal{V}_i$ represents a region whose boundary is given by: (1) set of points at the maximum sensing range from p_i; (2) set of points located on the boundary with another cell; (3) sets of points belonging to an obstacle. In the first case, the boundary is an arc of circle, hence the radius $r_i^{\mathcal{S}_i \cap \mathcal{V}_i}(\theta)$ is a constant function of θ. In the second case, following the same properties of Voronoi cells, the boundary is given by a segment, hence $r_i^{\mathcal{S}_i \cap \mathcal{V}_i}(\theta)$ is a continuous

function of θ. In the third case, the obstacle boundary is described by a sequence of arbitrarily curved segments. Notice that the connection between the different (curved or straight) segments (generated by either another cell or by obstacles) makes the function $r_i^{\mathcal{S}_i\cap\mathcal{V}_i}(\theta)$ continuous in θ, although not differentiable, since the condition in (11) holds with an equality (see Fig. 5 for β_1). However, given the visibility set definition (8), there may exists points $q \in \mathcal{V}_i$ such that q lies in the sensing range, i.e., $\|q - p_i\| \leq r_{s,i}$, but $\exists\gamma_1, \gamma_2 \in [0, 1]$, $\gamma_2 > \gamma_1$, verifying: (i) $p_i - \gamma\,(p_i - q) \notin \mathcal{O}\ \forall 0 \leq \gamma \leq \gamma_1$; (ii) $p_i - \gamma\,(p_i - q) \in \mathcal{O}$, $\forall\gamma_1 < \gamma \leq \gamma_2$; (iii) $p_i - \gamma\,(p_i - q) \notin \mathcal{O}$, for $\gamma_2 < \gamma \leq 1$. We define as $\overline{\mathcal{S}}_i$ as the set of all points q satisfying the properties above (the blind spot in Fig. 5). The set $\overline{\mathcal{S}}_i$ is said to be adjacent to $\mathcal{S}_i$ if $\exists q \in \overline{\mathcal{S}}_i$ and $\exists g \in \mathbb{R}^2$ such that $q + \varepsilon g \in \mathcal{S}_i$ for any arbitrary small $\varepsilon > 0$. When the $\overline{\mathcal{S}}_i$ and $\mathcal{S}_i$ are adjacent, the boundary between them is by construction given by a segment starting in p_i and touching both sets. Let this segment have angular polar coordinate β_2 (see Fig. 5). Assume, without loss of generality, that the obstacle is found for polar coordinates larger than β_2. While $r_i^{\mathcal{S}_i\cap\mathcal{V}_i}(\beta_2^+)$ is determined by the obstacle, either $r_i^{\mathcal{S}_i\cap\mathcal{V}_i}(\beta_2^-)$ is equal to the sansing range $r_{s,i}$ (as in Fig. 5) or it is defined by another Voronoi cell (or by another obstacle). In any of this cases $r_i^{\mathcal{S}_i\cap\mathcal{V}_i}(\beta_2^-) - r_i^{\mathcal{S}_i\cap\mathcal{V}_i}(\beta_2^+)$ is equal to the length of the boundary between $\overline{\mathcal{S}}_i$ and $\mathcal{S}_i$, which is non-null if the two sets are adjacent. The last point to discuss to end the proof is if it can be the case that $\overline{\mathcal{S}}_i$ is not adjacent to $\mathcal{S}_i$. This situation occurs if the obstacle splits apart the set $\mathcal{V}_i$, as in the case of a wall delimiting two rooms. However, this is not a blind spot since, by the arguments presented earlier, $r_i^{\mathcal{S}_i\cap\mathcal{V}_i}(\theta)$ is continuous in θ (i.e., the obstacle boundary is entirely visible). □

Using Proposition 1, we can now prove the following coverage Theorem.

Theorem 3 (*Coverage Test*)**.** *The coverage of the environment, in the case of homogeneous sensor ranges, is reached if* $\forall i = 1, \ldots, n$, $r_i^{\mathcal{S}_i\cap\mathcal{V}_i}(\theta) < r_{s,i}$, $\forall\theta \in [0, 2\pi)$, *and condition* (11) *does not hold true.*

Proof. If $r_i^{\mathcal{S}_i\cap\mathcal{V}_i}(\theta) < r_{s,i}$, $\forall\theta \in [0, 2\pi)$, $\forall i$, it implies that $q \in \mathcal{B}(\mathcal{S}_i \cap \mathcal{V}_i)$, either $q \in \mathcal{B}(\mathcal{S}_j \cap \mathcal{V}_j)$, with $j \neq i$, or $q \in \mathcal{B}(\mathcal{S}_i \cap \mathcal{V}_i)$ is on an obstacle contour (i.e., there is not any uncovered areas for each cell contour).

In order to achieve complete coverage of the environment, we have to show that for all i, all the points in $\mathcal{V}_i \setminus \mathcal{O}$ are visible. The fact that condition (11) never holds allows us to rule out the existence of blind spots. We have therefore to exclude the case in which $\overline{\mathcal{S}}_i$ is not adjacent to $\mathcal{S}_i$. Let us assume, by contradiction, that the set $\overline{\mathcal{S}}_i$ is not covered by any other agent $j \neq i$. However, being the mission space $\mathcal{Q}$ connected, there exists a free path in the mission space from p_i to $\overline{\mathcal{S}}_i$. Therefore, there exists at least one agent j such that $r_j^{\mathcal{S}_j\cap\mathcal{V}_j}(\theta) = r_{s,j}$ for some θ, i.e., whose cell contour reaches the sensing range, which contradicts the hypothesis. Hence, the proof. □

We want to remark that Theorem 3 holds true only for the case of homogeneous sensing ranges, i.e., by considering the set $\mathcal{S}_i \cap \mathcal{V}_i$. By accounting for the set $\mathcal{S}_i \cap \mathcal{H}_i$ there can be cases where a cell boundary touches neither another agent's cell, nor an obstacle or its sensing radius, as is shown in Fig. 3-b, hence we cannot say anything about coverage.

The accomplishment of full coverage is an information that can be decided solely at the team level, hence information exchange protocols are needed. Therefore, conditions for message exchanges, i.e. the maintenance of global connectivity, is unavoidable. In the next section, we will show that even this problem can be solved in the proposed framework.

3.6. Connectivity maintenance

We propose here a novel technique for connectivity maintenance between agents by using the proposed framework. The focus here is on the motion strategy that allows the system to preserve the connectivity constraints imposed by a topology controller. The latter is assumed to be an external component and is not in the scope of this paper. In the following, we assume that agent i can communicate with agent j if: 1. their distance is smaller than the communication range $R_{c,i}$, 2. there are not obstacles in between them (the agents are in line-of-sight). Further, for the sake of simplicity and without loss of generality, we assume a communication range $r_{c,i} \leq R_{c,i}$ that is equal to the sensing range $R_{s,i}$ (indeed, typically $R_{c,i} \gg R_{s,i}$). Our strategy to preserve connectivity is to modify the cell geometry in order to guarantee that two connected agents will remain so. To this end, let us define the set

$$\mathcal{M}_i = \left\{ \mathcal{S}_i \cap \bigcap_{j\in\underline{\mathcal{N}}_i} \mathcal{S}_j^\star \right\}, \tag{12}$$

where $\underline{\mathcal{N}}_i \subseteq \mathcal{N}_i$ is a subset of the i-th neighbour set, while $\mathcal{S}_j^\star$ is the same as $\mathcal{S}_j$ in (8) where $r_{s,j} = r_{c,j}$. If each agent follows the centroid computed on $\mathcal{M}_i$, we force the agents to stay within the visibility set of the neighbours, thus guaranteeing connectivity maintenance (for undirected graphs), as reported in the next Theorem.

Theorem 4 (*Connectivity Maintenance 1.*)**.** *Given a communication topology where* $r_{c,i} = R_{s,i} = R_s$, $\forall i$, *if the agent network is connected at the initial time* $t = 0$ *(i.e. there are no detached subnetworks) and each agent is subjected to the controlled dynamics* $\dot{p}_i(\mathcal{M}_i)$ *with* $k_e = 0$ *as defined in* (5), *the network will remain connected* $\forall t \geq 0$.

Proof. The i-th agent velocity $\dot{p}_i(\mathcal{M}_i)$ in (5) determines $p_i(t) \in \mathcal{M}_i$. By the definition in (12), we have $\mathcal{M}_i \subseteq \mathcal{S}_i$ and $\mathcal{M}_i \subseteq \mathcal{S}_j^\star$. It follows that the i-th agent is constrained to move inside the intersection between its visible set and the visible set (communication set) of the j-th agent, with $j \in \underline{\mathcal{N}}_i$. Since we are assuming $r_{c,i} = R_{s,i} = R_s$, the same result holds for all the agents, hence the proof. □

The previous result assumes that all agents have the same communication range. This assumption can be relaxed, by using a more general version of (12):

$$\underline{\mathcal{M}}_i = \left\{ \mathcal{S}_i \cap \bigcap_{j\in\underline{\mathcal{N}}_i} \underline{\mathcal{S}}_j^{\star,i} \right\}, \tag{13}$$

where $\underline{\mathcal{S}}_j^{\star,i}$ is computed as in (8) but replacing $r_{s,j}$ with $\underline{r}_{c,i,j} = \min\{r_{c,i}, r_{c,j}\}$. By using this modified set, we can generalise Theorem 4:

Corollary 5 (*Connectivity Maintenance 2.*)**.** *Given a communication topology where* $r_{c,i} = R_{s,i}$, *if the agent network is connected at the initial time* $t = 0$ *(i.e. there is no detached subnetworks) and each agent is subjected to the controlled dynamics* $\dot{p}_i(\underline{\mathcal{M}}_i)$ *with* $k_e = 0$ *as defined in* (5), *the network will remain connected for any time* $t \geq 0$.

Proof. By considering $\underline{\mathcal{M}}_i$ in (13), the same proof of Theorem 4 can be derived. □

The connectivity maintenance enforcement strategy discussed above can be thought of as a "module" that can be combined with other control tasks. For instance, by simply intersecting the

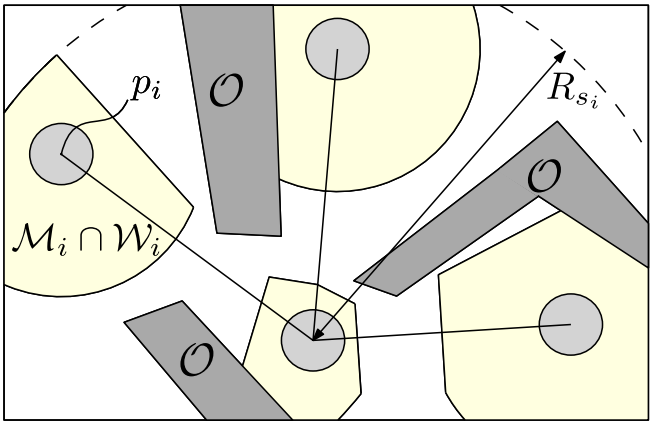

Fig. 6. Representation of the set $\mathcal{M}_i \cap \mathcal{W}_i$ defined in (12) (7).

set in (12) with (7) and adopting the definition of the controller dynamics $\dot{p}_i\left(\mathcal{M}_i \cap \tilde{\mathcal{V}}_i\right)$ with $k_e = 0$ in (5), we can obtain coverage and connectivity maintenance at the same time, while ensuring obstacle and collision avoidance. The same holds true for the heterogeneous case. Fig. 6 shows an example of this construction. Other applications are shown in the next section.

Remark 2 (*Performance*)**.** As previously presented, the connectivity constraint set $\mathcal{M}_i$ can be used directly to compute the centroid position and then the control law. However, especially in a coverage oriented application, the connectivity constraint may be stricter than necessary, and thus may affect the coverage performance. To overcome this issue we can compute the centroid over the cell without the intersection with the connectivity set $\mathcal{M}_i$, and then select the velocity to constrain the i-th agent's motion within the set $\mathcal{M}_i \cap \tilde{\mathcal{V}}_i$. This can be achieved by choosing $\dot{p}_i(\mathcal{S}_i \cap \tilde{\mathcal{V}}_i, \mathcal{M}_i \cap \tilde{\mathcal{V}}_i)$ and $k_e = 0$ in (5).

By adopting the proposed change, the hypotheses of Theorem 4 are not violated: the system is able to maintain connectivity, minimising the effect of the connectivity constraint, hence improving the performance in fulfilling the assigned task. The performance improvement is paid in terms of robustness, since small localisation uncertainties may easily lead to failures.

Theorem 6 (*Convergence Towards the Centroid*)**.** *The convergence towards the centroid position is guaranteed imposing $\dot{p}_i(\mathcal{A}_i)$ in (5) with $k_e = 0$, if two conditions are satisfied: 1. $\partial\mathcal{A}_i = \{p_i + r_i^{\mathcal{A}_i}(\theta)[\cos\theta \;\; \sin\theta]^T\}_{\theta=0}^{2\pi}$ and 2. the centroid falls inside the cell at any time i.e., $C_{\mathcal{A}_i} \in \mathcal{A}_i$.*

Proof. Condition 1. guarantees the existence of a straight path, which belongs to the cell and connects each point in the cell to the agent's position p_i, i.e., $p_i - \gamma(p_i - q) \in \mathcal{A}_i, \forall\gamma \in [0, 1], \forall q \in \mathcal{A}_i$. This condition is trivially satisfied for every convex set i.e., $\mathcal{V}_i, \tilde{\mathcal{V}}_i, \mathcal{H}_i, \tilde{\mathcal{H}}_i$, for the visibility set $\mathcal{S}_i$ (see Proposition 1) and for all the possible intersections between them. If also Condition 2. is satisfied, it means that there exist a straight path, which belongs to the cell $\mathcal{A}_i$ and connects the agent's position p_i with the centroid position $C_{\mathcal{A}_i}$. Hence, by applying $\dot{p}_i(\mathcal{A}_i)$ in (5) with $k_e = 0$ the agent converges towards the centroid position, since $J_{\text{cov}}(p, \mathcal{A})$ is still a valid Lyapunov function (see (4)), as the constraint in (5), under these conditions, is never active. The convergence to the centroid is a consequence of the LaSalle's invariance principle. □

Notice that Condition 2. may be not satisfied when the cell is non-convex, for pathological cases (e.g., it may happen by considering the cell $\mathcal{M}_i$). However, even in this case, safety and connectivity maintenance are secured by the constraint on the velocity selection in (5). If the problem occurs in the case of static coverage with connectivity maintenance, we should consider to increase the number of agents or to use a dynamic coverage algorithm (discussed in the next section).

4. Controlling the position of the centroid

In the distributed control algorithms described in Section 3, we have used a constant density function $\varphi_i(q)$ in (1), i.e. all the points in the $\mathcal{Q}$ space have the same weight. Therefore, the changes in the positions of the centroid and hence in the motion of the agents are solely dictated by geometric constraints. In this section, we will show how to use $\varphi_i(q)$ as an additional degree of freedom to move the centroid. By imposing time-varying density function $\varphi_i(q)$, we can address a new class of control problems in the same framework.

As a preliminary observation, since we are considering a time-varying density function, the derivative of the Lyapunov function $J_{\text{cov}}(p, \mathcal{A})$ in (1) is no more guaranteed to be negative. Indeed, its sign is in part determined by the variation in time of the density function:

$$\begin{aligned}\frac{d}{dt}J_{\text{cov}}(p, \mathcal{A}) &= \sum_{i=1}^{n} \frac{\partial}{\partial p_i}J_{\text{cov}}(p, \mathcal{A})\dot{p}_i + \frac{\partial}{\partial t}J_{\text{cov}}(p, \mathcal{A}) = \\ &= -2k_p \sum_{i=1}^{n} m_i \left\|p_i - C_{\mathcal{A}_i}\right\|^2 + \sum_{i=1}^{n} \int_{\mathcal{A}_i} \|q - p_i\|^2 \frac{\partial\varphi(q, t)}{\partial t} dq = \\ &= \sum_{i=1}^{n} \Gamma_i.\end{aligned} \tag{14}$$

This issue, however, has no significant impact for the class of algorithms presented next, because they do not require asymptotic convergence. In the following we omit the time dependence in the notation for clarity, i.e., $\phi(q, t) = \phi(q)$.

4.1. Dynamic coverage through exploration in non-convex spaces

As aforementioned, the ability to statically cover an area is related to the number of agents, to their sensing ranges, to their initial conditions and to the geometry of the mission space. An obvious precondition is that the sum of all the areas covered by the agents' sensing ranges be larger than the area of the mission space. If this condition is violated, static coverage is not possible, no matter the algorithm we use. If the precondition is satisfied, we can apply the techniques proposed in Section 3, and use *a-posteriori* the test in Theorem 3. If the test fails, we cannot decide if the coverage is complete. In both cases, we can opt for dynamic coverage. Informally speaking, while for static coverage we require that each point is always statically covered by at least one agent, for dynamic coverage we require that is covered by at least one agent *at some time instant*. Let us consider the homogeneous sensing range case with obstacle and collision avoidance capability i.e., let us consider the i-th cell $\tilde{\mathcal{W}}_i = \mathcal{S}_i \cap \tilde{\mathcal{V}}_i$. With respect to the previous section, dynamic coverage can be achieved by setting $k_e > 0$ in (5), i.e. considering the additional term that generates an exploratory behaviour, whose definition requires the construction of the Perturbed Voronoi Visibility set $\tilde{\mathcal{W}}_{i,\eta}$, where $\eta \ll r_{s,i}$ is a positive random variable. The set $\tilde{\mathcal{W}}_{i,\eta}$ is constructed by taking the interior of the boundary $\mathcal{B}(\tilde{\mathcal{W}}_{i,\eta}) = \{p_i + (r_i^{\tilde{\mathcal{W}}_i}(\theta) - \eta)[\cos\theta \;\; \sin\theta]^T\}_{\theta=0}^{2\pi}$. The exploratory control law $\dot{p}_i(\tilde{\mathcal{W}}_{i,\eta})$ is hence defined as in (5). If the total sensed area covered

by the agents is smaller than the mission space, the presence of $k_p > 0$ only produces configurations in which the agents are spaced out of a sufficient amount and then remain still (i.e., they stabilise on the fixed centroid positions). The addition of the derivative exploration term given by $k_e > 0$ generates inertia, which makes the agent prolong its motion along the direction of the centroid until it interacts with an obstacle or with other agents. To avoid periodic behaviours (e.g., the agent periodically goes back and forth along the same direction), we inject the random noise term η, which reshapes the geometry of the cells and avoids the repetition of the same motion patterns for the centroid.

This behaviour ensures the coverage of a larger area over time than with a static approach, but it does not guarantee that the motion will be oriented towards unexplored areas (e.g., an agent could never be pushed through a narrow hallway). This is what we called memoryless robots, i.e., we do not keep trace of the visited areas.

The ability of the system to visit unexplored areas can be significantly improved by giving memory of visited positions to each agent, and in particular, by combining the control law $\dot{p}_i(\tilde{\mathcal{V}}_{i,\eta})$ (5) with a non-uniform and time-varying function $\varphi_i(q)$, which depends on the past position of the i-th agent. Let $\mathcal{Q}_i(t)$ represent the portion of the mission space known to the i-th agent at time t. Contrary to the work of Cortes et al. [2], the function $\varphi_i(q)$ is no longer a probability distribution but it simply weighs the knowledge of the environment about the point q. When the point is unknown, it takes the maximum value $\overline{\varphi}_i$. When the point is discovered and remains within the sensing range of the agent, the function decreases exponentially. Finally, when the point goes out of sight, the knowledge decreases, hence $\varphi_i(q)$ increases exponentially back to the asymptotic value $\overline{\varphi}_i$. The resulting function is defined as follows:

$$\dot{\varphi}_i(q) = \begin{cases} -k_d\varphi_i(q), & \text{if } q \in \mathcal{S}_i, \\ k_u(\overline{\varphi}_i - \varphi_i(q)), & q \in \mathcal{Q}_i(t) \setminus \mathcal{S}_i \\ \overline{\varphi}_i & q \in \mathcal{Q} \setminus \mathcal{Q}_i(t). \end{cases} \tag{15}$$

The k_d constant quantifies the efficiency in gaining knowledge on a spot once it becomes visible, while k_u quantifies how quickly our information disappears when the point is no longer visible. Notably, a higher value of k_u pushes the agent to return soon to a visited place, while a lower value of k_u pushes it towards the exploration of new places. As a final observation, the efficiency of exploration and monitoring improves if the information on the visited place is shared among the agents, i.e., if the explored maps $\mathcal{Q}_i(t)$ and the $\varphi_i(q)$ functions are shared in a unified $\mathcal{Q}(t)$ and $\varphi(q)$, thus building a group of robots with memory of past positions and exchanging information. In this case, the connectivity maintenance strategy described in Section 3.6 can be used to guarantee a reliable connection between the agents.

4.2. Navigation

The centroid position can be modified to ensure group navigation, which, as mentioned before, can be subdivided into flocking and formation control. Since in both cases the agents are required to follow a sequence of way-points, the rationale is to let the centroid converge towards each way-point in the sequence. The proposed solution can enforce a flocking or a formation behaviour or even a switching behaviour. Notice that the Lloyd algorithm used for navigation is crucial to coordinate the agents and avoid collisions between them; by simply following the way-point sequence, the agents would avoid static obstacles but there would be no guarantee of avoiding collisions between agents.

The main idea is once again to act on the $\varphi_i(q)$ function in order to move the position of the centroid. Let $\bar{p}_i$ represent the current goal the i-th agent have to reach. We use the following exponential expression for $\varphi_i(q)$:

$$\varphi_i(q) = \begin{cases} \kappa_i \exp\left(-\frac{\|q-\bar{p}_i\|}{\rho_i}\right) & \text{if } q \in \mathcal{A}_i \\ 0 & \text{otherwise.} \end{cases} \tag{16}$$

The function is centred on the goal, κ_i is the normalisation factor to ensure that $\varphi_i(q)$ is a properly defined pdf, while ρ_i is a spreading factor that, intuitively, quantifies the relative importance of the goal. Indeed, if $\rho_i \to \infty$, all the points in the mission space have the same weight (as in the coverage case), while if $\rho_i \to 0$ the weight is concentrated on $\bar{p}_i$, thus attracting the centroid on $\bar{p}_i$. The spreading factor has the following dynamics

$$\dot{\rho}_i(\mathcal{A}_i) = \begin{cases} -\rho_i, & \text{if } \|C_{\mathcal{A}_i} - p_i\| < d_{i,\min} \\ -(\rho_i - \rho_i^D), & \text{otherwise,} \end{cases} \tag{17}$$

where $d_{i,\min}$ is a threshold value for the distance between the centroid and the actual agent position p_i, ρ_i^D is the desired spreading factor, and $\mathcal{A}_i$ is a generic i-th agent cell. The rationale of (17) is to avoid configurations in which the centroid stabilises on a point different from $\bar{p}_i$, generating a deadlock condition.

As a result, convergence guarantees can only be given by making strong assumptions. Under the sufficient condition that $\bar{p}_i, C_{\mathcal{A}_i} \in \mathcal{A}_i \, \forall t$, with $\partial\mathcal{A}_i = \{p_i + (r_i^{\mathcal{A}_i}(\theta))[\cos\theta \;\; \sin\theta]^T\}_{\theta=0}^{2\pi}$, the agent is guaranteed to reach the goal as shown by Theorem 7, which is based on results in the following proposition.

Proposition 2. *Assuming the variation of $C_{\mathcal{A}_i}$ due to the variation of $\mathcal{A}_i$ is negligible with respect to the variation of $C_{\mathcal{A}_i}$ due to (17), then for any set $\mathcal{A}_i$ the following holds true: $\frac{d\|C_{\mathcal{A}_i}-\bar{p}_i\|}{dt} < 0$ when $\|C_{\mathcal{A}_i}(t) - p_i\| < d_{i,\min}$, while $\frac{d\|C_{\mathcal{A}_i}-\bar{p}_i\|}{dt} \geq 0$ otherwise.*

Proof. We start by recalling the centroid definition, i.e.,

$$C_{\mathcal{A}_i} = \frac{\int_{\mathcal{A}_i} q\varphi(q)dq}{\int_{\mathcal{A}_i} \varphi(q)dq}$$

We can rewrite

$$C_{\mathcal{A}_i}(t) = \frac{\int_{\mathcal{A}_i}(z+\bar{p}_i)\kappa_i \exp(-\frac{\|z\|}{\rho_i(t)})}{\int_{\mathcal{A}_i} \varphi(q)dq}dz,$$

by recalling that $\int_{\mathcal{A}_i} \varphi(q)dq = 1$, we have

$$\|C_{\mathcal{A}_i}(t) - \bar{p}_i\| = \left\| \frac{\int_{\mathcal{A}_i} z\kappa_i \exp(-\frac{\|z\|}{\rho_i(t)})}{\int_{\mathcal{A}_i} \varphi(q)dq}dz \right\|. \tag{18}$$

Let us now consider the time t when $\|C_{\mathcal{A}_i}(t) - p_i\| < d_{i,\min}$: in such a case, after $\delta t > 0$ seconds, we have that, under the effect of (17), $\rho_i(t+\delta t) = e^{-\delta t}\rho_i(t) = \alpha\rho_i(t)$, where $\alpha \in [0, 1)$. Since $0 \leq \rho_i(t+\delta t) < \rho_i(t) \leq \rho_i^D$, we have immediately by applying (18) to $\rho_i(t+\delta t)$ that $\|C_{\mathcal{A}_i}(t+\delta t) - \bar{p}_i\| < \|C_{\mathcal{A}_i}(t) - \bar{p}_i\|$. The same argument holds when $\|C_{\mathcal{A}_i}(t) - p_i\| \geq d_{i,\min}$ in (17), which concludes the proof. □

The following results are based on Proposition 2, thereby hinge on the assumption that the influence on the centroid position due to the variation of the cell geometry is negligible with respect to the variation of the centroid position induced by (17).

Theorem 7 (*Navigation 1*)**.** *Given $\bar{p}_i, C_{\mathcal{A}_i} \in \mathcal{A}_i \, \forall t$, with $\partial\mathcal{A}_i = \{p_i + (r_i^{\mathcal{A}_i}(\theta))[\cos\theta \;\; \sin\theta]^T\}_{\theta=0}^{2\pi}$, by applying the control law $\dot{p}_i(\mathcal{A}_i)$ with $k_e = 0$ as defined in (5) with the density function (16) and the spreading factor dynamics $\dot{\rho}_i(\mathcal{A}_i)$ in (17), it follows $p_i \to \bar{p}_i$.*

Proof. By assuming to be in the condition $\|p_i - C_{\mathcal{A}_i}\| \geq d_{i,\min}$, the value of ρ_i is constant (constant function (16)), thus the control

law $\dot{p}_i(\mathcal{A}_i)$ with $k_e = 0$ as defined in (5) ensures $p_i \to C_{\mathcal{A}_i}$, see Theorem 6. Hence, there exists a time instant t_1 such that $\|p_i(t_1) - C_{\mathcal{A}_i}(t_1)\| < d_{i,\min}$. According to (17), the value of ρ_i start decreasing and, as such, we may have that $\Gamma_i > 0$ in (14). In such a case, there may exist a time $t_2 > t_1$ such that $\|p_i(t_2) - C_{\mathcal{A}_i}(t_2)\| \geq d_{i,\min}$. However, we noticed that $\forall t \in [t_1, t_2]$, $C_{\mathcal{A}_i}(t)$ moves towards $\bar{p}_i$, as shown in Proposition 2, i.e., $\|C_{\mathcal{A}_i}(t_2) - \bar{p}_i\| < \|C_{\mathcal{A}_i}(t_1) - \bar{p}_i\|$, while $p_i(t)$ moves towards $C_{\mathcal{A}_i}(t)$. Hence, $\|p_i(t_2) - \bar{p}_i\| < \|p_i(t_1) - \bar{p}_i\|$. When $\|p_i(t) - C_{\mathcal{A}_i}(t)\| \geq d_{i,\min}$, $t > t_2$, $\rho_i(t) \to \rho_D$ by (17), hence there exists $t_3 > t_2$ such that $\|p_i(t_3) - C_{\mathcal{A}_i}(t_3)\| < d_{i,\min}$. By means of (5) and noticing that $\Gamma_i < 0$ in (14) $\forall t \in [t_2, t_3]$ (see Proposition 2), we have that $p_i(t) \to C_{\mathcal{A}_i}(t)$, $\forall t \in [t_2, t_3]$, therefore $\|p_i(t_3) - \bar{p}_i\| < \|p_i(t_2) - \bar{p}_i\|$. Since $\frac{\partial \|p_i(t) - \bar{p}_i\|}{\partial t} < 0$, $\forall t$, $\|p_i(t) - \bar{p}_i\|$ acts as a common Lyapunov function for the switching dynamic induced by (17), hence the asymptotic stability is proved. □

To reach locations that do not belong to the set $\mathcal{A}_i$, we plan an a-priori feasible path for each agent. By discretising the i-th planned path in way-points $\mathcal{WP}_i = \{wp_i^1, wp_i^2, \ldots, wp_i^m\}$, given the agent position p_i, and assuming wp_i^k the closest way-point to p_i, we select as active way-point $wp_i^{k+l_i}$ which is the point ahead of a preview length l_i with respect to wp_i^k. The preview length l_i is a generic function of the visibility set of the robot. Since we assume to have planned a safe path for each robot, i.e., a path composed of a sequence of elementary path segments that link the starting agents' positions $\mathcal{P}$ with the goal positions $\mathcal{E}$ and do not intersect any obstacle in the set $\mathcal{O}$, we can assert that there always exist a value for the preview length l_i such that $wp_i^{k+l_i} \in \mathcal{A}_i$ (at least, $l_i = 1$). Hence by centring the density function on the active way-point, we are able to steer the robot towards the goal.

Theorem 8 (*Navigation 2*)**.** *By applying the control law $\dot{p}_i(\mathcal{A}_i)$ with $k_e = 0$ in (5), $\partial\mathcal{A}_i = \{p_i + (r_i^{\mathcal{A}_i}(\theta))[\cos\theta \;\; \sin\theta]^T\}_{\theta=0}^{2\pi}$ and with the density function (16), assuming 1. $C_{\mathcal{A}_i} \in \mathcal{A}_i$ and 2. $\bar{p}_i = wp_i^{k+l_i}$ belong to the discretised path $\mathcal{WP}_i = \{wp_i^1, wp_i^2, \ldots, wp_i^m\}$ and to the set $\mathcal{A}_i$, and 3. that the spreading factor dynamics $\dot{\rho}_i(\mathcal{A}_i)$ is given by (17), then we have $p_i \to wp_i^m$.*

Proof. By Theorem 7, the distance $\|p_i - wp_i^{k+l_i}\| \to 0$. The new active way-point, assuming constant preview length $l_i = 1$ to simplify the notation, becomes wp_i^{k+2}. Since the existence of a new reachable way-point is ensured because the path planned is assumed to be safe, $wp_i^{k+l_i} \to wp_i^m$, hence the proof. □

The *flocking* behaviour can be achieved by combining the navigation strategy just explained and the connectivity maintenance strategy. The *formation* behaviour, where each agent has to keep constant the distance from each other along the motion, is obtained combining the navigation strategy, the connectivity maintenance strategy and by imposing virtual radii $\tilde{\Delta}_{ij}$, equal to the desired formation distance to be used in (6) for collision avoidance. Let us define $\tilde{\Delta}_{ij} = \underline{R}_{c,i,j} - \chi$, where $\underline{R}_{c,i,j} = \min\{R_{c,i}, R_{c,j}\}$, by adjusting the parameter $\chi > 0$ we can control the group behaviour. In fact, assigning small values to χ, we are imposing a rigid formation configuration, and the allowable distance $d_{a,ij}$ between the i-th and the j-th agent becomes $\underline{R}_{c,i,j} - \chi < d_{a,ij} < \underline{R}_{c,i,j}$. On the contrary when $\chi = \underline{R}_{c,i,j} - \Delta_{ij}$, where $\Delta_{ij} = \delta_i + \delta_j$ is the physical encumbrance of the agents, we fall in the flocking case i.e., we are allowing for a flexible formation.

Remark 3. In a multi-agent navigation, the condition $\bar{p}_i \in \mathcal{A}_i$, $\forall t$, is a quite strong assumption. In fact, the condition does not hold true when $\bar{p}_i \in \mathcal{A}_j$, but this does not imply that the agent remains in a deadlock condition. Indeed, the simulations and the experimental results in Sections 5, 6 show convergence to the goal positions despite the violation of this sufficient condition. This is an important evidence of the fact that this condition it is only sufficient (quite conservative) and not necessary. We want also to point out that the intersection of the considered set, e.g., $\tilde{\mathcal{W}}_i$, with the set $\mathcal{M}_i$ in (12), used for flocking and formation behaviour, does not guarantee anymore the sufficient condition $\partial\mathcal{A}_i = \{p_i + (r_i^{\mathcal{A}_i}(\theta))[\cos\theta \;\; \sin\theta]^T\}_{\theta=0}^{2\pi}$; in fact in some pathological cases, this condition does not hold true, hence we cannot ensure convergence.

4.3. Rendezvous in non-convex spaces

For the rendezvous problem, two of the presented strategies have to be combined together. The connectivity of the system has to be guaranteed and at the same time the agents position have to converge to the same location. The connectivity can be guaranteed by applying Theorem 4, the convergence behaviour instead can be ensured by Theorem 7. In particular, let us select $\varphi_i(q)$ as in (16), where $\bar{p}_i$ is the closest point to the mean of the neighbouring positions that belongs to the i-th agent cell. By using the set $\mathcal{M}_i$ in (12), the controlled dynamics $\dot{p}_i(\mathcal{M}_i)$ with $k_e = 0$ in (5), the weighting function (16) and the spreading factor dynamics $\dot{\rho}_i(\mathcal{M}_i)$ in (17), the agents rendezvous is ensured. To prove it, we first introduce the following definition.

Definition 1. A topological space $\mathcal{Q}$ is simply connected (or 1-connected) if no holes are passing all the way through it.

We are now in a position to prove the following Theorem.

Theorem 9 (*Rendezvous 1*)**.** *Consider a non-convex simply connected space, a visibility dependent graph topology $\mathcal{G}$, and assume that the agent network is connected at the initial time $t = 0$ (i.e. there is no detached subnetworks). By applying: 1. the dynamics $\dot{p}_i(\mathcal{M}_i)$ with $k_e = 0$ in (5), 2. the density function (16) with*

$$\bar{p}_i = \sum_{j \in \mathcal{N}_i} p_j / card(\mathcal{N}_i),$$

which satisfies

$$p_i - \gamma(p_i - \bar{p}_i) \in \mathcal{M}_i, \forall \gamma \in [0, 1], \tag{19}$$

3. the centroid position that satisfies

$$p_i - \gamma(p_i - C_{\mathcal{M}_i}) \in \mathcal{M}_i, \forall \gamma \in [0, 1] \tag{20}$$

and 4. the spreading factor $\dot{\rho}_i(\mathcal{M}_i)$ in (17), each agent will converge to the same single position.

Proof. Since the communication graph is connected for all $t > 0$ (Theorem 4), the communication between the i-th and the neighbouring j-th agent ($\forall j \in \mathcal{N}_i$) is guaranteed. By using $\dot{p}_i(\mathcal{M}_i)$ with the density function (16) and a spreading factor following $\dot{\rho}_i(\mathcal{M}_i)$ in (17), each agent converges asymptotically towards its $\bar{p}_i$ by means of Theorem 7 (indeed, $\|p_i(t) - \bar{p}_i\|$ acts as a common Lyapunov function for the switching dynamic induced by (17)). Notice that (19), (20) ensures that $\bar{p}_i, C_{\mathcal{M}_i} \in \mathcal{M}_i$ and that there exists a straight path that links p_i with $\bar{p}_i$ and $C_{\mathcal{M}_i}$. Since the means $\bar{p}_i$ are updated in due course, $\forall i$, they follows a linear consensus-like dynamic. If visibility among the agents is complete, $\bar{p}_i = \sum_{j=1}^{n} p_j/n$, $\forall i = 1 \ldots n$ and convergence is enforced by Theorem 7.

Otherwise, we have to account for the dynamics of $\bar{p}_i$. We first recall that restricting to non-convex simply connected environments, the agents do not encircle any obstacle. Therefore, the communication topology does not define any cyclic path around an obstacle. As a consequence, if there is partial visibility, due to

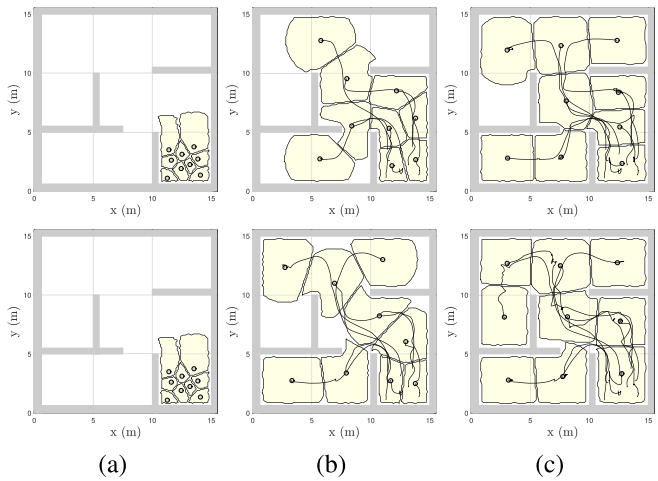

Fig. 7. Simply connected environment with 9 agents (faded circles). Top row: snapshots at time $t_0 = 0$ s (a), $t_1 = 3.3$ s, (b), and $t_2 = 9.09$ s (c) of the static coverage simulation. Bottom row: snapshots at time $t_0 = 0$ s (a), $t_1 = 3.3$ s, (b), and $t_2 = 7.26$ s (c) of the adaptive coverage simulation. Yellow regions represent the agents' cells with $R_{s,i} = 3.0$ m. (For interpretation of the references to colour in this figure legend, the reader is referred to the web version of this article.)

the fact that the communication is undirected, it is also rooted. In such a case, $\bar{p}_i$ is equal to the average position of its visibility set. By means of $\dot{p}_i(\mathcal{M}_i)$, we have $p_i(t) \to \bar{p}_i$, hence the i-th leaf agent converges to the average position of its visibility set by means of Theorem 7 applied locally. Along with the convergence, the average point $\bar{p}_i$ is continuously updated and moves towards the root. Due to this continuous convergence, there exists $\bar{t}$ such that for $t > \bar{t}$ all the agents are in view of the root, i.e., $\bar{p}_i$ coincides with the root $\forall i$, therefore complete visibility is enforced, Theorem 7 applies and hence the proof. □

Notice that also in this case the conditions (19) (20) are sufficient and not necessary conditions.

By manipulating the communication topology we are also able to assert convergence in more complex situations. Indeed, we can ensure rendezvous in a generic non-convex space if the graph topology, on which we compute the agent cells (12), is fixed, connected acyclic and undirected. This assumption allows rendezvous also in cluttered environments, not only in a non-convex simply connected space, as described next.

Corollary 10 (*Rendezvous 2*)**.** *A sufficient condition to guarantee rendezvous in a generic non-convex environment is the existence of a fixed connected acyclic undirected communication topology.*

Proof. By considering a fixed connected acyclic undirected graph the communication topology cannot by definition encircle obstacles in the map, thus the proof of Theorem 9 applies directly. □

5. Simulation results

The proposed approach has been extensively tested in simulations. In the following we show simulation results for the algorithms described in the previous sections.

5.1. Static coverage vs Adaptive static coverage

From the simulations, it has been empirically observed that there are obstacle configurations not allowing static coverage using the algorithm in Section 3.2. In this cases, we show that, apart

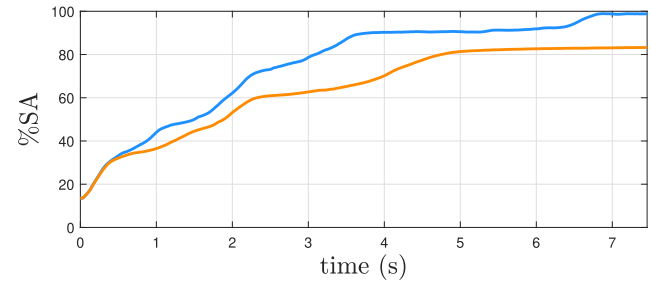

Fig. 8. Percentage of the sensed area (SA) versus time. Comparison between the simulations in Fig. 7: in orange the static coverage, in blue the adaptive static coverage. (For interpretation of the references to colour in this figure legend, the reader is referred to the web version of this article.)

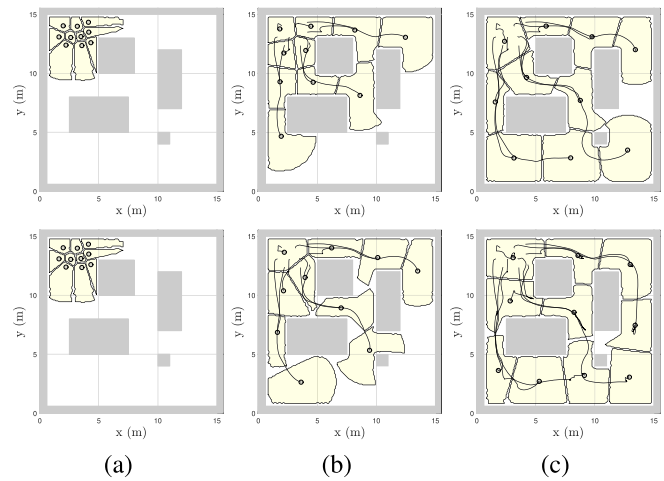

Fig. 9. Non-convex cluttered environment with 10 agents (faded circles). Top row: snapshots at time $t_0 = 0$ s (a), $t_1 = 1.32$ s, (b), and $t_2 = 5.94$ s (c) of the static coverage simulation. Bottom row: snapshots at the same time instants of the adaptive coverage simulation. Yellow regions represent the agents' cells with $R_{s,i} = 3.0$ m. (For interpretation of the references to colour in this figure legend, the reader is referred to the web version of this article.)

from increase the number of agents or increase the $r_{s,i}$ ranges, full coverage can be achieved by using the adaptive coverage presented in Section 3.4. In Fig. 7 we compare qualitatively the static coverage and the adaptive static coverage for the same initial conditions and in the same environment (simply connected environment). Fig. 8 depicts quantitatively the level of coverage percentage versus time. Both qualitatively and quantitative it can be notice how the adaptive static coverage achieves full coverage, while the static coverage is stuck in a local minimum. In Figs. 9 and 10 we provide further evidence for a cluttered environment, with similar results.

5.2. Memoryless exploration vs intelligent exploration

Fig. 11 reports the comparison of the explored areas for the memoryless exploration (a), the exploration with memory of past positions (b) and for the exploration with memory of past positions and exchanging information between agents (c) after $t = 16.5$ s. The graphs report in blue the gained knowledge measured with $\varphi(q)$, whose dynamic is reported in (15). A darker colour represents a lower value (higher knowledge), while yellow areas are the value associate to the maximum $\overline{\varphi}_i$ (no knowledge). The corresponding quantitative analysis is offered in Fig. 12 representing the accumulated sensed area (ASA) percentage, confirming the efficiency of the memory-based solutions.

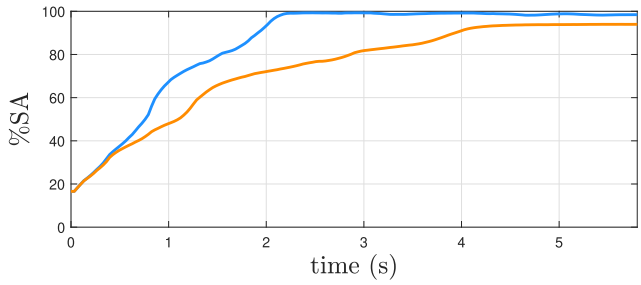

Fig. 10. Percentage of the sensed area (SA) versus time. Comparison between the simulations in Fig. 9: in orange the static coverage, in blue the adaptive static coverage. (For interpretation of the references to colour in this figure legend, the reader is referred to the web version of this article.)

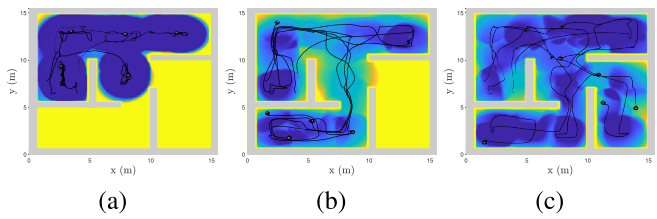

Fig. 11. Snapshots at time $t = 16.5$ s of the memoryless exploration (a), exploration with memory of past positions (b) and exploration with memory of past positions and exchanging information (c) of a non-convex environment with 5 agents (faded circles) with $r_{s,i} = 2$ m. We depict in yellow the unexplored areas with value $\overline{\varphi}_i$. (For interpretation of the references to colour in this figure legend, the reader is referred to the web version of this article.)

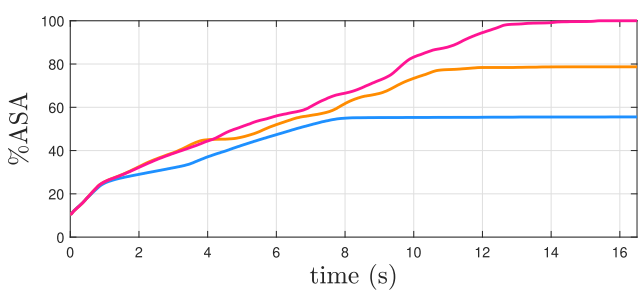

Fig. 12. Percentage of the accumulated sensed area (ASA) versus time. Comparison between the simulations in Fig. 11: (a) blue, (b) orange, (c) pink. (For interpretation of the references to colour in this figure legend, the reader is referred to the web version of this article.)

5.3. Rendezvous in non-convex space

The effectiveness of the rendezvous algorithm is tested in two different conditions. First, an ideal scenario where agents are assumed to be points is considered. Hence, we impose $\dot{p}_i(\mathcal{M}_i)$, ignoring collision between agents and rendezvous is reached with each agent converging to the same point. Fig. 13 reports both qualitative and quantitative results. In particular, the sum of the norm of the difference between the agents' position and the mean of the agents' positions in time (rendezvous error) is used as quantitative metric, which, in this ideal case, converges to zero. In a realistic case, instead, collision avoidance is active, i.e. the centroid position is computed on the set $\tilde{\mathcal{M}}_i = \left\{\tilde{\mathcal{V}}_i \cap \mathcal{S}_i \cap \bigcap_{j\in\underline{\mathcal{N}}_i} \mathcal{S}_j^\star\right\}$. For empirical evidence, we use two additional scenarios, reported in Fig. 14 with three snapshots: in the top row, the case of a connected non-convex environment with a visibility-based communication graph topology (starting from a connected configuration): in the bottom row, the case of a non-convex cluttered environment where we keep the communication graph fixed in time, connected acyclic and undirected to satisfy the hypotheses of Corollary 10. The quantitative analysis by means of the rendezvous errors versus time (Fig. 15) clearly show convergence towards a fixed value dictated by the agents encumbrance.

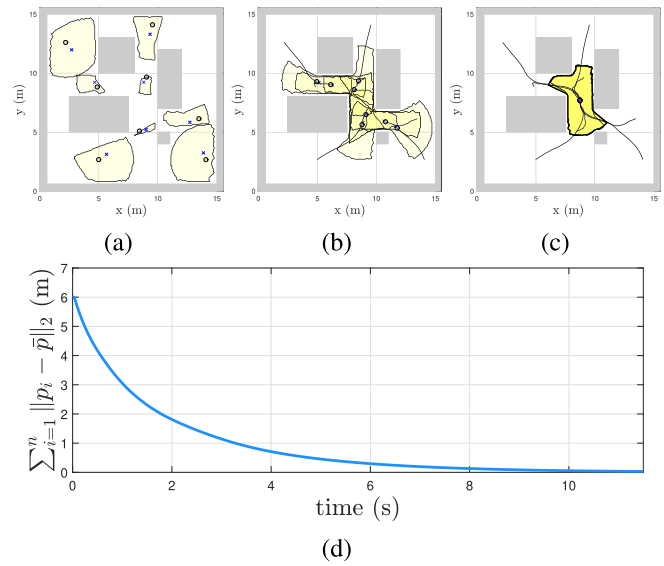

Fig. 13. Ideal rendezvous simulation in non-convex cluttered environment, where the graph topology is fixed and satisfy the properties in Corollary 10. Snapshots at time $t_0 = 0$ s (a), $t_1 = 1.15$ s, (b), and $t_2 = 11.55$ s (c) are reported, where the yellow areas represent $\mathcal{W}_i$ defined in (12), blue crosses indicate the centroid positions $C_{\mathcal{M}_i}$, $r_{s,i} = 3$ m, $r_{c,i} = 2r_{s,i}$. (d) sum of the norm of the rendezvous errors versus time. (For interpretation of the references to colour in this figure legend, the reader is referred to the web version of this article.)

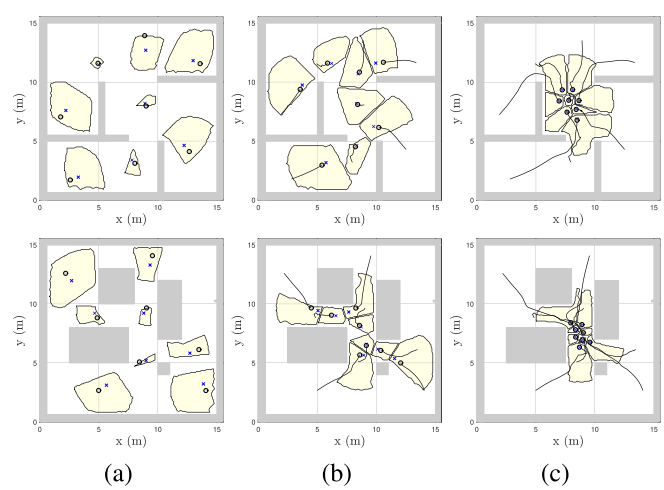

Fig. 14. Rendezvous simulations. Top row: non-convex simply connected environment with 8 agents (faded circles) with snapshots at time $t_0 = 0$ s (a), $t_1 = 0.66$ s, (b), and $t_2 = 2.31$ s (c). Bottom row: non-convex cluttered environment with snapshots at time $t_0 = 0$ s (a), $t_1 = 0.99$ s, (b), and $t_2 = 3.96$ s (c). The yellow areas are points belonging to $\tilde{\mathcal{M}}_i = \left\{\tilde{\mathcal{V}}_i \cap \mathcal{S}_i \cap \bigcap_{j\in\underline{\mathcal{N}}_i} \mathcal{S}_j^\star\right\}$, blue crosses indicate the centroid positions $C_{\tilde{\mathcal{M}}_i}$, $r_{s,i} = 3$ m, $r_{c,i} = 2r_{s,i}$. (For interpretation of the references to colour in this figure legend, the reader is referred to the web version of this article.)

5.4. Navigation: flocking vs formation control

Simulations for the navigation task are reported in Fig. 16, for both the formation case (top row) and the flocking case

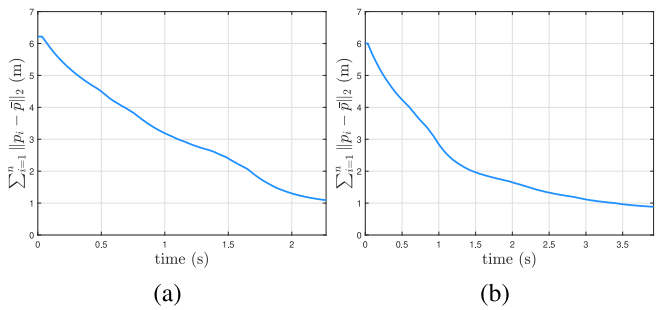

Fig. 15. Rendezvous errors for the upper (a) and bottom (b) scenarios of Fig. 14.

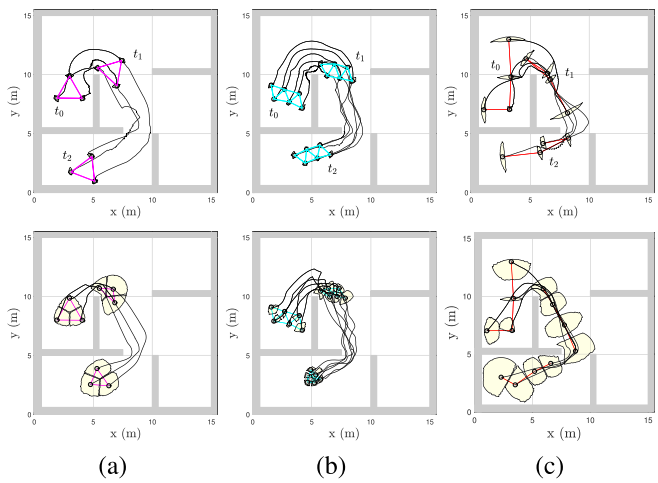

Fig. 16. Six navigation task simulations. Top row: three simulation results of the formation control algorithm, each figure depicts three snapshots in different time instants. Bottom row: the same scenarios addressed by the flocking algorithm. The link between the agents represent the edges considered by the connectivity maintenance policy.

(bottom row). Three different simulations for each approach are reported. For all the simulations, we keep the graph topology time invariant. In Figs. 16-a and 16-b we have the homogeneous case, i.e., R_s is equal for all the agents, and two isostatic topology configurations (minimally rigid configurations), while in 16-c we consider the heterogeneous case with a flexible topology configuration (non-rigid). We recall that the number of maintenance link in a minimally rigid topology configuration with n agents in $\mathbb{R}^2$ is equal to $2n-3$: if we have more links, we fall in a redundantly rigid topology configuration; otherwise, if we have less links between agents, we have a flexible topology configuration [54].

In Fig. 17 we depict quantitative results from the simulation in Fig. 16-a. In particular, Fig. 17-a shows the distances between agents (solid lines) and the limits imposed by the collision avoidance with virtual agent dimensions $\tilde{\Delta}_{ij}$ (bottom dashed line) and the minimum sensing range $\underline{R}_{s,i,j}$ (top dashed line) for the formation control case. As it can be noticed, the constraints are always satisfied. Instead, Fig. 17-b reports similar results for the flocking case, which is constrained between the real agent dimensions Δ_{ij} (bottom dashed line) and the minimum sensing range $\underline{R}_{s,i,j}$ (top dashed line).

6. Experimental results

In this Section, we provide experimental evidence to practically prove the feasibility and the effectiveness of the unified Lloyd-based distributed control law (5). We present here the rendezvous and the flocking algorithms with three unicycle-like

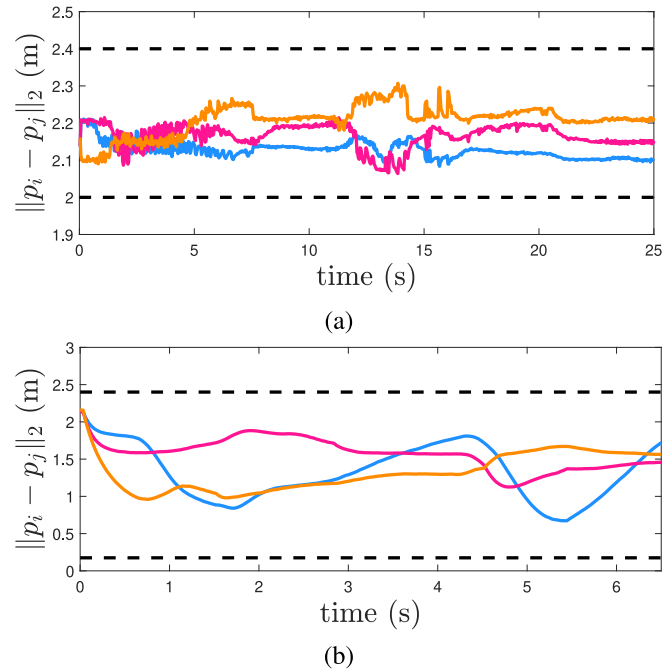

Fig. 17. Distances between agents for the simulation reported in Fig. 16, on the top the formation case, on the bottom the flocking case.

robots, developed at the University of Trento, in a non-convex environment. The results obtained from the experiments are consistent with the simulated evidences presented in Section 5 for all the different control goals enumerated in Section 2.1. To account for the nonholonomic constraints of the unicycle dynamics, we used the controller introduced in [55] and re-adapted in [56]. Figs. 18 and 19 depict three time instants for the rendezvous and flocking algorithms. In both the experiments the robots respect safety, the imposed connectivity constraints and converge towards the goal. In these experiments we select as topology control strategy the one proposed in [56].

Fig. 20 and Fig. 21 report the rendezvous error and the distances between agents for the experiments in Figs. 18 and 19 respectively, thus resembling Fig. 20 and Fig. 17 of Section 5.

From these graphs it is evident the nice accordance between simulations and experiments. In the attached multimedia material we show some video of the experiments illustrated in Figs. 18, 19.

7. Conclusions

We proposed a unified Lloyd-based framework for multi-agent systems able to deal with static and dynamic coverage, connectivity maintenance, rendezvous, flocking and formation control in complex environments and in a distributed fashion. To validate our approach, we provide theoretical foundations, simulation and experimental evidences. In the near future we plan to define necessary conditions for the convergence of the navigation and rendezvous algorithms, and to validate experimentally all the proposed algorithm by increasing the number of robots. Moreover, we plan to analyse the system behaviour under robot failures, delays in communication or cyber attacks.

Declaration of competing interest

The authors declare that they have no known competing financial interests or personal relationships that could have appeared to influence the work reported in this paper.

Fig. 18. Rendezvous in non-convex environment with three robots. We picked three significant instant of time of the experiment.

Fig. 19. Flocking in non-convex environment with three robots. We picked three significant instant of time of the experiment.

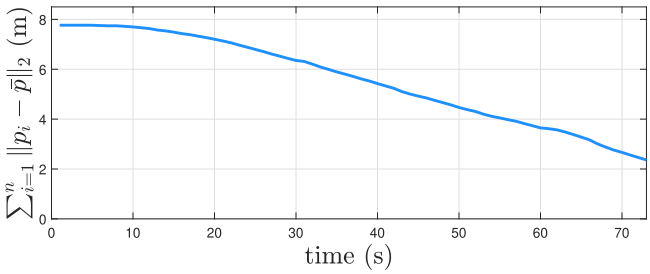

Fig. 20. Rendezvous errors for the experiment reported in Fig. 18.

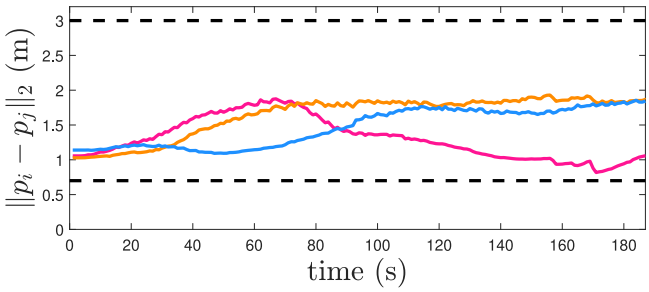

Fig. 21. Distances between agents for the experiments reported in Fig. 19.

Appendix A. Supplementary data

Supplementary material related to this article can be found online at https://doi.org/10.1016/j.robot.2022.104207.

References

[1] T. Vicsek, A question of scale, Nature 411 (6836) (2001) 421.

[2] J. Cortes, S. Martinez, T. Karatas, F. Bullo, Coverage control for mobile sensing networks, IEEE Trans. Robot. Autom. 20 (2) (2004) 243–255.

[3] S. Lloyd, Least squares quantization in PCM, IEEE Trans. Inform. Theory 28 (2) (1982) 129–137.

[4] A. Breitenmoser, M. Schwager, J.-C. Metzger, R. Siegwart, D. Rus, Voronoi coverage of non-convex environments with a group of networked robots, in: 2010 IEEE International Conference on Robotics and Automation, IEEE, 2010, pp. 4982–4989.

[5] L.C. Pimenta, V. Kumar, R.C. Mesquita, G.A. Pereira, Sensing and coverage for a network of heterogeneous robots, in: 2008 47th IEEE Conference on Decision and Control, IEEE, 2008, pp. 3947–3952.

[6] Y. Stergiopoulos, M. Thanou, A. Tzes, Distributed collaborative coverage-control schemes for non-convex domains, IEEE Trans. Automat. Control 60 (9) (2015) 2422–2427.

[7] M. Boldrer, D. Fontanelli, L. Palopoli, Coverage control and distributed consensus-based estimation for mobile sensing networks in complex environments, in: 2019 IEEE 58th Conference on Decision and Control, CDC, IEEE, 2019, pp. 7838–7843.

[8] Y. Kantaros, M. Thanou, A. Tzes, Distributed coverage control for concave areas by a heterogeneous robot–swarm with visibility sensing constraints, Automatica 53 (2015) 195–207.

[9] L. Lu, Y.-K. Choi, W. Wang, Visibility-based coverage of mobile sensors in non-convex domains, in: 2011 Eighth International Symposium on Voronoi Diagrams in Science and Engineering, IEEE, 2011, pp. 105–111.

[10] A. Howard, M.J. Matarić, G.S. Sukhatme, Mobile sensor network deployment using potential fields: A distributed, scalable solution to the area coverage problem, in: Distributed Autonomous Robotic Systems, Vol. 5, Springer, 2002, pp. 299–308.

[11] M. Boldrer, F. Riz, F. Pasqualetti, L. Palopoli, D. Fontanelli, Time-inverted Kuramoto dynamics for κ-clustered circle coverage, in: IEEE Conference on Decision and Control, CDC, IEEE, 2021, pp. 1205–1211.

[12] W. Li, C.G. Cassandras, Distributed cooperative coverage control of sensor networks, in: Proceedings of the 44th IEEE Conference on Decision and Control, IEEE, 2005, pp. 2542–2547.

[13] M. Andreetto, M. Pacher, D. Macii, L. Palopoli, D. Fontanelli, A distributed strategy for target tracking and rendezvous using uavs relying on visual information only, Electronics (ISSN: 2079-9292) (10) (2018) http://dx.doi.org/10.3390/electronics7100211, [Online]. Available: URL http://www.mdpi.com/2079-9292/7/10/211.

[14] B. Yamauchi, A frontier-based approach for autonomous exploration, in: Cira, Vol. 97, 1997, p. 146.

[15] B. Yamauchi, Frontier-based exploration using multiple robots, in: Proceedings of the Second International Conference on Autonomous Agents, 1998, pp. 47–53.

[16] W. Burgard, M. Moors, C. Stachniss, F.E. Schneider, Coordinated multi-robot exploration, IEEE Trans. Robot. 21 (3) (2005) 376–386.

[17] A. Franchi, L. Freda, G. Oriolo, M. Vendittelli, The sensor-based random graph method for cooperative robot exploration, IEEE/ASME Trans. Mechatronics 14 (2) (2009) 163–175.

[18] J.S. Cepeda, L. Chaimowicz, R. Soto, J.L. Gordillo, E.A. Alanís-Reyes, L.C. Carrillo-Arce, A behavior-based strategy for single and multi-robot autonomous exploration, Sensors 12 (9) (2012) 12772–12797.

[19] S.H. Semnani, O.A. Basir, Semi-flocking algorithm for motion control of mobile sensors in large-scale surveillance systems, IEEE Trans. Cybern. 45 (1) (2014) 129–137.

[20] M. Schwager, F. Bullo, D. Skelly, D. Rus, A ladybug exploration strategy for distributed adaptive coverage control, in: 2008 IEEE International Conference on Robotics and Automation, IEEE, 2008, pp. 2346–2353.

[21] D. Haumann, V. Willert, K.D. Listmann, DisCoverage: from coverage to distributed multi-robot exploration, IFAC Proc. Vol. 46 (27) (2013) 328–335.

[22] A. Okabe, B. Boots, K. Sugihara, S.N. Chiu, Spatial Tessellations: Concepts and Applications of Voronoi Diagrams, Vol. 501, John Wiley & Sons, 2009.

[23] C. Franco, D.M. Stipanović, G. López-Nicolás, C. Sagüés, S. Llorente, Persistent coverage control for a team of agents with collision avoidance, Eur. J. Control 22 (2015) 30–45.
[24] A. Mellone, G. Franzini, L. Pollini, M. Innocenti, Persistent coverage control for teams of heterogeneous agents, in: 2018 IEEE Conference on Decision and Control, CDC, IEEE, 2018, pp. 2114–2119.
[25] N. Zhou, X. Yu, S.B. Andersson, C.G. Cassandras, Optimal event-driven multi-agent persistent monitoring of a finite set of targets, in: 2016 IEEE 55th Conference on Decision and Control, CDC, IEEE, 2016, pp. 1814–1819.
[26] S.L. Smith, M. Schwager, D. Rus, Persistent robotic tasks: Monitoring and sweeping in changing environments, IEEE Trans. Robot. 28 (2) (2011) 410–426.
[27] F. Pasqualetti, A. Franchi, F. Bullo, On cooperative patrolling: Optimal trajectories, complexity analysis, and approximation algorithms, IEEE Trans. Robot. 28 (3) (2012) 592–606.
[28] M. Boldrer, F. Pasqualetti, L. Palopoli, D. Fontanelli, Multiagent persistent monitoring via time-inverted kuramoto dynamics, IEEE Control Systems Letters 6 (2022) 2798–2803.
[29] L. Sabattini, N. Chopra, C. Secchi, Decentralized connectivity maintenance for cooperative control of mobile robotic systems, Int. J. Robot. Res. 32 (12) (2013) 1411–1423.
[30] M.C. De Gennaro, A. Jadbabaie, Decentralized control of connectivity for multi-agent systems, in: Proceedings of the 45th IEEE Conference on Decision and Control, IEEE, 2006, pp. 3628–3633.
[31] E. Stump, A. Jadbabaie, V. Kumar, Connectivity management in mobile robot teams, in: 2008 IEEE International Conference on Robotics and Automation, IEEE, 2008, pp. 1525–1530.
[32] Y. Kim, M. Mesbahi, On maximizing the second smallest eigenvalue of a state-dependent graph Laplacian, in: Proceedings of the 2005, American Control Conference, 2005, IEEE, 2005, pp. 99–103.
[33] M. Schuresko, J. Cortés, Distributed motion constraints for algebraic connectivity of robotic networks, J. Intell. Robot. Syst. 56 (1–2) (2009) 99–126.
[34] M.M. Zavlanos, G.J. Pappas, Controlling connectivity of dynamic graphs, in: Proceedings of the 44th IEEE Conference on Decision and Control, IEEE, 2005, pp. 6388–6393.
[35] M.M. Zavlanos, M.B. Egerstedt, G.J. Pappas, Graph-theoretic connectivity control of mobile robot networks, Proc. IEEE 99 (9) (2011) 1525–1540.
[36] M.M. Zavlanos, G.J. Pappas, Distributed connectivity control of mobile networks, IEEE Trans. Robot. 24 (6) (2008) 1416–1428.
[37] C.W. Reynolds, Flocks, Herds and Schools: A Distributed Behavioral Model, Vol. 21, no. 4, ACM, 1987.
[38] R. Olfati-Saber, Flocking for multi-agent dynamic systems: Algorithms and theory, IEEE Trans. Automat. Control 51 (3) (2006) 401–420.
[39] H. Ando, Y. Oasa, I. Suzuki, M. Yamashita, Distributed memoryless point convergence algorithm for mobile robots with limited visibility, IEEE Trans. Robot. Autom. (ISSN: 2374-958X) 15 (5) (1999) 818–828, http://dx.doi.org/10.1109/70.795787.
[40] J. Lin, A. Morse, B. Anderson, The multi-agent rendezvous problem. An extended summary, in: Cooperative Control, Springer, 2005, pp. 257–289.
[41] J. Cortés, S. Martínez, F. Bullo, Robust rendezvous for mobile autonomous agents via proximity graphs in arbitrary dimensions, IEEE Trans. Automat. Control 51 (8) (2006) 1289–1298.
[42] D.V. Dimarogonas, K.J. Kyriakopoulos, On the rendezvous problem for multiple nonholonomic agents, IEEE Trans. Automat. Control 52 (5) (2007) 916–922.
[43] M. Ji, M. Egerstedt, Distributed coordination control of multiagent systems while preserving connectedness, IEEE Trans. Robot. 23 (4) (2007) 693–703.
[44] A. Ganguli, J. Cortés, F. Bullo, Multirobot rendezvous with visibility sensors in nonconvex environments, IEEE Trans. Robot. 25 (2) (2009) 340–352.
[45] X. Li, D. Sun, J. Yang, Preserving multirobot connectivity in rendezvous tasks in the presence of obstacles with bounded control input, IEEE Trans. Control Syst. Technol. 21 (6) (2012) 2306–2314.
[46] D. Zhou, Z. Wang, S. Bandyopadhyay, M. Schwager, Fast, on-line collision avoidance for dynamic vehicles using buffered voronoi cells, IEEE Robot. Autom. Lett. 2 (2) (2017) 1047–1054.
[47] S.G. Lee, Y. Diaz-Mercado, M. Egerstedt, Multirobot control using time-varying density functions, IEEE Trans. Robot. 31 (2) (2015) 489–493.
[48] M. Boldrer, L. Palopoli, D. Fontanelli, Lloyd-based approach for robots navigation in human-shared environments, in: IEEE/RSJ International Conference on Intelligent Robots and Systems, IEEE/RSJ, 2020 pp. 6982–6989.
[49] M. Boldrer, A. Antonucci, P. Bevilacqua, L. Palopoli, D. Fontanelli, Multi-agent navigation in human-shared environments: A safe and socially-aware approach, Robot. Auton. Syst. (2021) 103979.
[50] J. Jahn, Introduction to the Theory of Nonlinear Optimization, Springer Nature, 2020.
[51] O. Arslan, D.E. Koditschek, Voronoi-based coverage control of heterogeneous disk-shaped robots, in: 2016 IEEE International Conference on Robotics and Automation (ICRA), IEEE, 2016, pp. 4259–4266.
[52] F. Aurenhammer, Power diagrams: properties, algorithms and applications, SIAM J. Comput. 16 (1) (1987) 78–96.
[53] A. Kwok, S. Martinez, Deployment algorithms for a power-constrained mobile sensor network, Int. J. Robust Nonlinear Control IFAC-Affiliated J. 20 (7) (2010) 745–763.
[54] L. Asimow, B. Roth, The rigidity of graphs, Trans. Amer. Math. Soc. 245 (1978) 279–289.
[55] M. Boldrer, M. Andreetto, S. Divan, L. Palopoli, D. Fontanelli, Socially-aware reactive obstacle avoidance strategy based on limit cycle, IEEE Robot. Autom. Lett. 5 (2) (2020) 3251–3258.
[56] M. Boldrer, P. Bevilacqua, L. Palopoli, D. Fontanelli, Graph connectivity control of a mobile robot network with mixed dynamic multi-tasks, IEEE Robot. Autom. Lett. 6 (2) (2021) 1934–1941.

Manuel Boldrer received the master's degree in Mechatronic Engineering and Ph.D degree in Materials, Mechatronics and Systems Engineering from the University of Trento, Trento, Italy, respectively in 2018 and 2022. He was a Visiting Scholar at the University of California, Riverside, Riverside, US, in 2021. As of today, he is a Postdoctoral Researcher with the Cognitive Robotics Department (CoR), Delft University of Technology, Delft, The Netherlands, in the Reliable Robot Control Lab. His research interests include mobile robotics and distributed coordination of multi-agent systems.

Luigi Palopoli received the Ph.D. degree in computer engineering from the Scuola Superiore S. Anna, Pisa, Italy, in 2002. He is currently a Professor of Robotics and Real-Time Embedded Systems with the University of Trento, Trento, Italy. His past research revolved around real-time control systems and control with computation and communication constraints. Recently, he has shifted his interest towards robotics and coordinated two large European initiatives in the area of robots for elderly assistance. Prof. Palopoli is currently an Associate Editor for the IEEE Transactions on Automatic Control and the Elsevier Journal of Systems Architecture.

Daniele Fontanelli (M'10, SM'19) received the M.S. degree in Information Engineering in 2001, and the Ph.D. degree in Automation, Robotics and Bioengineering in 2006, both from the University of Pisa, Pisa, Italy. He was a Visiting Scientist with the Vision Lab of the University of California at Los Angeles, Los Angeles, US, from 2006 to 2007. From 2007 to 2008, he has been an Associate Researcher with the Interdepartmental Research Center "E. Piaggio", University of Pisa. From 2008 to 2013 he joined as an Associate Researcher the Department of Information Engineering and Computer Science and from 2014 the Department of Industrial Engineering, both at the University of Trento, Trento, Italy, where he is now an Associate Professor. He has authored and co-authored more than 150 scientific papers in peer-reviewed top journals and conference proceedings. He is currently an Associate Editor for the IEEE Transactions on Instrumentation and Measurement and for the IET Science, Measurement & Technology Journal. From 2018 he is also an Associate Technical Program Committee Member for the IEEE/RSJ International Conference on Intelligent Robots and Systems. From 2021 he si appointed as Associate Editor in Chief for the IEEE Transactions on Instrumentation and Measurement. His research interests include distributed estimation and control, human localisation algorithms, synchrophasor estimation, clock synchronisation algorithms, real-time estimation and control, resource aware control, wheeled mobile robots control and service robotics.